$H-Al-CH_3$ from CH_4 and Al would be 34 kcal exothermic.[17]

We conclude that the primary species formed is $HAlCH_3$ (or $DAlCD_3$) on the basis of energetic considerations as well as comparing the observed ν_{Al-H} and δ_{CH_3} with known organoaluminum hydrides.

Photolysis of the deposited CH_4/Al and CD_4/Al matrices initially led to a slight increase in product bands but with simultaneous production of new bands. The new bands appear in regions similar to those reported for $(R_2AlH)_2$ and $(R_2AlCl)_2$ species (some differences would be expected since in the matrices "free" species would be present). The following scheme seems consistent:

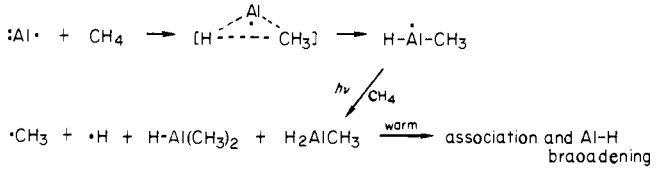

The most important question remains: "Why are Al atoms reactive (without photolysis) over other metal atoms?" Two considerations come to mind. First, Al-H and Al-C bonds are comparatively strong (68 and 66 kcal, respectively). Second, ground-state Al atoms are in a ^2P state ($3s^23p^1$), and it would be expected that Al atoms would possess reactive radical-like properties.[18,19] Also note that ground-state Al atoms are in the same electronic state as photoexcited Cu atoms, which are also reactive with CH_4 at 10 K.[7] It seems reasonable to conclude that Al atoms are able to react by a homolytic bond cleavage process, and the driving force is the formation of Al-H and Al-C bonds. The ^2P state appears to be uniquely reactive.

Experimental Section

The apparatus and procedures have been described in a previous publication.[8] The photolytic experiments were carried out for 1-, 2-, or 3-h periods by using a medium-pressure mercury UV lamp (140 W, unfiltered).

Acknowledgment. The donors of the Petroleum Research Fund, administered by the American Chemical Society, are acknowledged with gratitude.

Registry No. CH_4, 74-82-8; Al, 7429-90-5; Mg, 7439-95-4; Cu, 7440-70-2; Ti, 7440-32-6; Cr, 7440-47-3; Mn, 7439-96-5; Fe, 7439-89-6; Co, 7440-48-4; Ni, 7440-02-0; Pd, 7440-05-3; Cu, 7440-50-8; Ag, 7440-22-4; Au, 7440-57-5; Zn, 7440-66-6; Sn, 7440-31-5; Pb, 7439-92-1; Ga, 7440-55-3; In, 7440-74-6.

(17) Taking the Al-C bond as 66 and the Al-H bond as 68 with $H-CH_3$ as 104 kcal/mol; ref 14, p 95. "Handbook of Chemistry and Physics", 56th ed.; Weast, R. C., Ed.; CRC Press: Cleveland, OH, 1975-1976; pp F-224, F-215.

(18) Hertzberg, G. "Atomic Spectra and Atomic Structure"; Dover Publications: New York, 1944; pp 132, 140.

(19) For studies of Al atom-benzene interactions and related work, see: Kasai, P. H.; McLeod, D. *J. Am. Chem. Soc.* **1979**, *101*, 5860.

Coordinately Unsaturated Clusters. A Novel Catalytic Reaction

R. R. Burch,[†] A. J. Shusterman,[†] E. L. Muetterties,*[†] R. G. Teller,[‡] and Jack M. Williams*[‡]

Contribution from the Department of Chemistry, University of California, Berkeley, California 94720, and Chemistry Division, Argonne National Laboratory, Argonne, Illinois 60439. *Received October 20, 1982*

Abstract: The dinuclear rhodium hydride $\{(\mu\text{-H})Rh[P(O\text{-}i\text{-}C_3H_7)_3]_2\}_2$ is a catalyst precursor for stereoselective hydrogenation of dialkylalkynes and diarylalkynes to the corresponding *trans*-alkenes. Both H_2 and the alkyne compete for reaction with the dimer with the respective products being $(H)(\mu\text{-H})_3Rh_2[P(O\text{-}i\text{-}C_3H_7)_3]_4$ and $(\mu\text{-H})_2(\mu\text{-}\eta^2\text{-}RC_2R)Rh_2[P(O\text{-}i\text{-}C_3H_7)_3]_4$. The further reaction of the tetrahydride complex with alkyne and also the rearrangement of the η^2-alkyne complex yield a bridged vinyl derivative, $(\mu\text{-H})[\mu\text{-}\eta^2\text{-}RC{=}C(H)R]Rh_2[P(O\text{-}i\text{-}C_3H_7)_3]_4$, **3**, which has a trans arrangement of alkyl or aryl groups as established by X-ray crystallographic studies. The rate-determining step in the catalytic cycle appears to be hydrogen addition to the vinyl derivative. Competitive with hydrogen addition to the vinyl derivative is diarylalkyne addition and insertion to give the mononuclear complex $[R(H)C{=}C(R)(R)C{=}CR]Rh[P(O\text{-}i\text{-}C_3H_7)_3]_2$, which was also defined by an X-ray crystallographic study. The latter is a catalyst precursor for alkyne hydrogenation to form *cis*-alkenes. Dynamic stereochemical features of the vinyl complexes in the solution state are described as well as intermolecular alkyne exchange between free alkyne and the vinyl complexes.

Introduction

A major focus of our metal cluster research has been the design of coordinately unsaturated clusters, specifically clusters in which most or all of the metal atoms have open coordination sites. Presently, this class of clusters is comprised largely of the $(\mu\text{-H})RhL_2$ group in which the immediate coordination sphere of each rhodium(I) atom has a planar set of 2 H (bridging) and 2 L ligands.[1-9] These polynuclear rhodium hydrides are very active catalyst precursors for hydrogenation reactions,[3,9] and this cluster catalysis is the subject of this article.

Cluster catalysis[10,11] has a potential for chemoselective and stereoselective reactions that may be unavailable to mononuclear

[†] University of California.

[‡] Argonne National Laboratory.

(1) Day, V. W.; Fredrich, M. F.; Reddy, G. S.; Sivak, A. J.; Pretzer, W. R.; Muetterties, E. L. *J. Am. Chem. Soc.* **1977**, *99*, 8091.

(2) Brown, R. K.; Williams, J. M.; Fredrich, M. F.; Day, V. W.; Sivak, A. J.; Muetterties, E. L. *Proc. Natl. Acad. Sci. U.S.A.* **1979**, *76*, 2099.

(3) Sivak, A. J.; Muetterties, E. L. *J. Am. Chem. Soc.* **1979**, *101*, 4878.

(4) Muetterties, E. L.; Sivak, A. J.; Brown, R. K.; Williams, J. M.; Fredrich, M. F.; Day, V. W. "Fundamental Research in Homogeneous Catalysis"; Plenum Publishing: New York, 1972; Vol. 3, p 487.

(5) Brown, R. K.; Williams, J. M.; Sivak, A. J.; Muetterties, E. L. *Inorg. Chem.* **1980**, *19*, 370.

(6) Burch, R. R.; Muetterties, E. L.; Schultz, A. J.; Gebert, E. G.; Williams, J. M. *J. Am. Chem. Soc.* **1981**, *103*, 5517.

0002-7863/83/1505-3546$01.50/0

metal complexes by virtue of cooperativity between metal centers in a cluster. A simple reaction probe of chemoselectivity and stereoselectivity is alkyne hydrogenation. The hydrogenation product may be either an alkane or an alkene, and the alkene produced may have either cis or trans stereochemistry.

Mononuclear metal complexes that catalyze alkyne hydrogenation yield *cis*-alkenes. Formation of *trans*-alkenes is often observed but typically this is the consequence of an isomerization step involving the first-formed *cis*-alkene.[12a] Formation first of a *cis*-alkene is expected in an intermolecular hydrogenation of a disubstituted alkyne that is effected at a single metal atom: hydrogen atom transfer from the metal to a coordinated alkyne would yield a σ-vinylmetal complex with a cis orientation[12b-d] of the original alkyne substituent groups (eq 1), and barring a facile

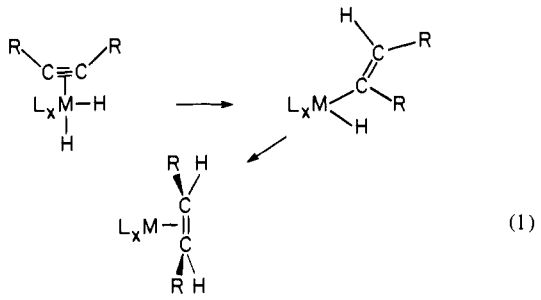

(1)

isomerization[13] of the *cis*-vinyl complex, the second intramolecular hydrogen atom transfer must yield a coordinated *cis*-alkene. In contrast, a catalytic alkyne hydrogenation reaction effected at two or more metal centers has the potential for *trans*-alkene formation,[12a] and an illustrative, although hypothetical, sequence is shown in eq 2. Until our recent findings,[9] this potential had not been realized. All reported alkyne hydrogenations using metal cluster catalyst precursors such as $(\eta^5\text{-}C_5H_5)_2Mo_2(CO)_4$[14] and $Ni_4(\mu_3\text{-}\eta^2\text{-}RC{\equiv}CR)_3(CNR)_4$[15] have yielded *cis*-alkenes although

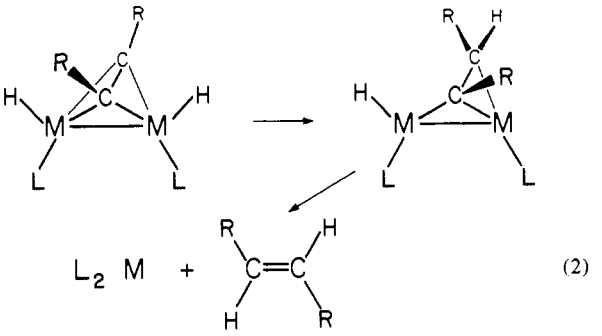

(2)

largely *trans*-alkene was reported[16] to form in the noncatalytic reaction of hydrogen with $Fe_2(CO)_6[\mu\text{-}\eta^2\text{-}(CH_3)_3CC{\equiv}CC(CH_3)_3]$.

We describe in this article a catalytic alkyne hydrogenation reaction,[9] based on a dinuclear metal complex catalyst precursor, that yields *trans*-alkenes and also the molecular features of the sequential steps that comprise the catalytic cycle. The catalyst precursor was $\{(\mu\text{-}H)Rh[P(O\text{-}i\text{-}C_3H_7)_3]_2\}_2$.

Experimental Section

Reagents and Solvents. All manipulations were carried out under an argon atmosphere in a Vacuum Atmospheres drybox or under a nitrogen atmosphere with use of conventional Schlenk techniques. Toluene, benzene, pentane, and tetrahydrofuran solvents were distilled from sodium benzophenone ketyl; 2-propanol and methanol were degassed prior to use. Toluene-d_8, benzene-d_6, and tetrahydrofuran-d_8 NMR solvents were purchased from Aldrich or from U.S. Services and were distilled from sodium benzophenone ketyl. Alkenes were purchased from Aldrich or from Chem Samples and were used without further purification except where otherwise indicated. 3-Hexyne and diphenylacetylene were used as received (Aldrich), and di-*p*-tolylacetylene was prepared by the literature procedure[17] and was a generous gift of Dr. K. D. Tau. 2-Butyne was purchased from Chem Samples, degassed by two freeze–evacuate–melt cycles, and was then vacuum distilled after a minimum of 1 week of storage over CaH_2. Hydrogen was used as received (Matheson).

Spectroscopic and Analytical Methods. Proton NMR spectra were recorded in toluene-d_8 solution at 180, 200, or 250 MHz on instruments using Oxford superconducting magnets interfaced with Nicolet 1180 computers. Chemical shifts (^1H) are reported relative to tetramethylsilane. ^{31}P NMR spectra were recorded in toluene-d_8 solution or in toluene-d_8/pentane mixtures at 72.9 MHz on the 180-MHz spectrometer with the chemical shifts reported relative to 85% H_3PO_4.

Chromatographic separations of volatile hydrocarbon products were effected with a Perkin-Elmer Sigma 3 instrument (flame ionization detector) employing either a 12 ft × $^1/_8$ in. 15% dimethylsulfolane on Chromosorb P column or a 12 ft × $^1/_8$ in. OV-17 column. Identification of compounds was confirmed by GC–MS analysis with a Finnigan 4000 instrument interfaced with a Finnigan INCOS data system (30-m SP 2250 (WCOT) column). Mass spectrometric analyses of the rhodium complexes were made with an AEI MS-12 instrument interfaced with an INCOS data system.

Microanalyses were carried out by Vazken H. Tashinian in the U.C. Berkeley Microanalytical Laboratory.

Preparation of $(\mu\text{-}H)[\mu\text{-}\eta^2\text{-}C_6H_5C{=}C(H)C_6H_5]Rh_2[P(O\text{-}i\text{-}C_3H_7)_3]_4$ (3a) and $(\mu\text{-}H)[\mu\text{-}\eta^2\text{-}CH_3C_6H_4C{=}C(H)C_6H_4CH_3]Rh_2[P(O\text{-}i\text{-}C_3H_7)_3]_4$ (3b). In a typical procedure, 0.020 g (0.019 mmol) of $\{(\mu\text{-}H)Rh[P(O\text{-}i\text{-}C_3H_7)_3]_2\}_2$[3,7] and 0.004 g (0.023 mmol) of diphenylacetylene were dissolved in approximately 5 mL of toluene. The resulting solution was stirred for 1 h at room temperature. The the toluene was removed by vacuum distillation. The residue was dissolved in pentane and cooled to −40 °C to yield a crop of large red crystals, yield 0.016 g (70%). Anal. Calcd for $C_{50}H_{96}O_{12}P_4Rh_2$: C, 49.27; H, 7.94. Found: C, 49.96; H, 8.10. ^1H NMR (toluene-d_8, 20 °C, 250 MHz) δ +8.50 (d, J = 7.5 Hz, Ar CH, 2 H), +7.75 (d, J = 7.4 Hz, Ar CH, 2 H), +7.53 (t, $J_{Rh\text{-}H}$ = 5.4 Hz, $=CHC_6H_5$, 1 H), +7.0 (m, Ar CH, 6 H; this integral is corrected for solvent contributions), +5.1 (m, $CH(CH_3)_2$, 6 H), +4.4 (m, $CH(CH_3)_2$, 6H), +1.38 (d, J = 7.7 Hz, $CH(CH_3)_2$, 18 H), +1.35 (d, J = 7.7 Hz, $CH(CH_3)_2$, 18 H), +1.18 (d, J = 7.0 Hz, $CH(CH_3)_2$, 18 H), +1.02 (d, J = 7.0 Hz, $CH(CH_3)$, 18 H), −11.14 (ttt, $J_{Rh\text{-}H}$ = 20.5 Hz,

(7) Burch, R. R.; Muetterties, E. L.; Day, V. W. *Organometallics* **1982**, *1*, 188.

(8) (a) Meier, E. B., Burch, R. R.; Muetterties, E. L.; Day, V. W. *J. Am. Chem. Soc.* **1982**, *104*, 2661. (b) Kulzick, M. A.; Price, R. T.; Muetterties, E. L.; Day, V. W. *Organometallics* **1982**, *1*, 1256.

(9) Alkyne catalytic hydrogenation was described preliminarily in a communication: Burch, R. R.; Muetterties, E. L.; Teller, R. G.; Williams, J. M. *J.* Am. *Chem. Soc.* **1982**, *104*, 4257.

(10) Muetterties, E. L. *J. Organomet. Chem.* **1977**, *200*, 177.

(11) Muetterties, E. L. *Catal. Rev.-Sci. Eng.* **1981**, *23*, 69.

(12) (a) Muetterties, E. L. *Inorg. Chim. Acta* **1981**, *50*, 1. (b) This is the expectation for nonradical processes in which H_2 *adds to the metal center* initially. (c) Clark, H. C.; Wong, C. S. *J. Organomet. Chem.* **1975**, *92*, C31–34. In this reference is described a formation of the *cis*-vinyl complexes from $PtHX[P(C_2H_5)_3]_2$ and disubstituted acetylenes, but it was found that the reaction of the platinum hydride with $C_2(COOCH_3)_2$ with free-radical initiators (*J. Am. Chem. Soc.* **1977**, *99*, 7073–4) gives the *trans*-vinyl complex and it was concluded that the reaction involves radical intermediates. (d) Otsuka and Nakamura reported selective formation of a *trans*-vinyl complex in the addition of perfluorobutyne to $(C_5H_5)_2MH_n$ complexes (cf. discussion in the following: Otsuka, S.; Nakamura, A. *Adv. Organomet. Chem.* **1976** *14*, 254–5). There is the possibility that *cis*-vinyl formed first and was catalytically isomerized to the trans isomer.[13]

(13) There is also the possibility of a purely thermal isomerization of a mononuclear vinylmetal complex having a very low barrier to cis–trans isomerization. Isomerizations of such complexes have been reported, but only in one case was the possibility of a catalyzed isomerization established (note that cis–trans isomerization of olefins can be very fast due to catalysis by glass or traces of acid or base). For example, Huggins and Bergman (Huggins, J. M.; Bergman, R. G. *J. Am. Chem. Soc.* **1981**, *103*, 3002–3011) describe an insertion of alkyne into the Ni–CH_3 bond of methyl(2,4-pentanedionato)-(triphenylphosphine)nickel to give initially a *cis*-vinyl complex and conclude that $(C_6H_5)_3P$ catalyzes a cis–trans isomerization of this complex to give the *trans*-vinyl isomer. Hart and Swartz (Hart, D. W.; Swartz, J. *J. Organomet. Chem.* **1975**, *87*, C11–C14) report that $CH_3RhI(CO)(PR_3)_2$(*cis*-vinyl) complexes resulting from the alkyne addition to the corresponding hydride complex slowly isomerize to the *trans*-vinyl isomer at ~20 °C in benzene solution. They found the rate to be unaffected by acids, bases, or radical inhibitors and concluded that the isomerization was intramolecular. The extensive set of platinum–vinyl complexes studied by Clark and Wong[12c] did not exhibit facile cis–trans vinyl isomerization reactions in solution.

(14) Slater, S.; Muetterties, E. L. *Inorg. Chem.* **1980**, *19*, 3337.

(15) Muetterties, E.; Band, E.; Kokorin, A.; Pretzer, W. R.; Thomas, M. G. *Inorg. Chem.* **1980**, *19*, 1552.

(16) Muetterties, E. L.; Pretzer, W. R.; Thomas, M. G.; Beier, B. F.; Thorn, D. L.; Day, V. W.; Anderson, A. B. *J. Am. Chem. Soc.* **1978**, *100*, 2090.

(17) Cope, A. C.; Smith, D. S.; Cotter, R. J. "Organic Syntheses"; Wiley: New York, 1963; Collective Vol. IV, p 377.

J_{P-H} = 73.4 Hz, 14.4 Hz, RhHRh, 1 H; this hydride resonance collapsed to a triplet, J_{Rh-H} = 20.5 Hz, in the $^1H\{^{31}P\}$ NMR spectrum at +20 °C); $^{31}P\{^1H\}$ NMR (20 °C) +136.5 (br, $\omega_{1/2}$ = 42 Hz), +132.5 ppm (br, $\omega_{1/2}$ = 42 Hz).

Red crystals of $(\mu\text{-H})[\mu\text{-}\eta^2\text{-}CH_3C_6H_4C{=}C(H)C_6H_4CH_3]Rh_2[P(O\text{-}i\text{-}C_3H_7)_3]_4$ were similarly prepared by the reaction of $\{(\mu\text{-H})Rh[P(O\text{-}i\text{-}C_3H_7)_3]_2\}_2$ with di-*p*-tolylacetylene; ^1H NMR (toluene-d_8, 20 °C, 250 MHz) δ +8.45 (d, *J* = 7.7 Hz, Ar CH, 2 H), +7.65 (d, *J* = 7.7 Hz, Ar CH, 2 H), +7.55 (t, J_{Rh-H} = 4.2 Hz, $=CHC_6H_4CH_3$, 1 H), +6.9 (m, Ar CH, 4 H, this integral is corrected for solvent contributions), +5.1 (m, $CH(CH_3)_2$, 6 H), +4.5 (m, $CH(CH_3)_2$, 6 H), +2.17 (s, Ar CH_3, 3 H), +2.12 (s, Ar CH_3, 3 H), +1.38 (d, *J* = 3.0 Hz, $CH(CH_3)_2$, 18 H), +1.32 (d, *J* = 3.0 Hz, $CH(CH_3)_2$, 18 H), +1.08 (d, *J* = 7.4 Hz, $CH(CH_3)_2$, 18 H), +0.98 (d, *J* = 7.4 Hz, $CH(CH_3)_2$, 18 H), -11.15 (ttt, J_{Rh-H} = 20.1 Hz, J_{P-H} = 74.0 Hz, 14.8 Hz, RhHRh, 1 H); $^{31}P\{^1H\}$ NMR (20 °C) +136.5 (br s, $\omega_{1/2}$ = 40 Hz), +132.0 ppm (br s, $\omega_{1/2}$ = 40 Hz). The $^{31}P\{^1H\}$ NMR spectrum at −65 °C consisted of an uninterpretable complex array of resonances ranging in chemical shift from +128 to +159 ppm, arising from four inequivalent phosphorus nuclei.

The following procedure was used to obtain crystals of $(\mu\text{-H})[\mu\text{-}\eta^2\text{-}CH_3C_6H_4C{=}C(H)C_6H_4CH_3]Rh_2[P(O\text{-}i\text{-}C_3H_7)_3]_4$ suitable for X-ray crystallography. A bent glass tube of approximate volume 25 mL was charged with 0.010 g (0.010 mmol) of $\{(\mu\text{-H})[P(O\text{-}i\text{-}C_3H_7)_3]_2\}_2$, 0.02 g (0.10 mmol) of di-*p*-tolylacetylene, and 5 mL of degassed 2-propanol. The mixture was degassed by three freeze–evacuate–melt cycles and sealed under vacuum. The solids were dissolved by immersing the tube in a 40 °C water bath. Red crystals separated out as the solution was allowed to slowly cool. The crystals were isolated by inverting the tube so as to decant the 2-propanol and then sealing the tube between the liquid and the crystals.

Preparation of $(\mu\text{-H})[\mu\text{-}\eta^2\text{-}CH_3C{=}C(H)CH_3]Rh_2[P(O\text{-}i\text{-}C_3H_7)_3]_4$ (3c). In a typical procedure, 0.020 g (0.019 mmol) of $\{(\mu\text{-H})Rh[P(O\text{-}i\text{-}C_3H_7)_3]_2\}_2$ was dissolved in approximately 8 mL of toluene. An aliquot of the vapor (8.7 mL, ~0.25 mmol of 2-butyne) from a serum stopper-capped Schlenk flask containing a mixture of N_2 and 2-butyne (*p*(2-butyne) ~ 0.7 atm at 20 °C) was injected by means of a gas-tight syringe into the toluene solution, resulting in a nearly instantaneous change in the solution from dark green to orange-yellow. The toluene was removed by vacuum distillation after ~0.5 h. The resulting yellow residue was extracted with methanol. The solution was filtered through a fine-porosity frit, and the solvent volume was reduced by means of vacuum distillation to approximately 5 mL. The solution was cooled to −40 °C to yield a crop of orange-yellow crystals, which were isolated by filtration, washed with cold pentane, and dried under vacuum, yield 0.012 g (60%). Anal. Calcd for $C_{40}H_{92}O_{12}P_4Rh_2$: C, 43.88; H, 8.47; P, 11.32. Found: C, 43.46; H, 8.25; P, 11.37. ^1H NMR (toluene-d_8, 20 °C, 180 MHz) δ +5.95 (br m, $=CHCH_3$, 1 H), +5.15 (m, $CH(CH_3)_2$, 6 H), +4.90 (m, $CH(CH_3)_2$, 6 H), +2.65 (br m, vinyl CH_3, 3 H), +1.95 (d, *J* = 5.5 Hz, vinyl CH_3, 3 H), +1.30 (m, $CH(CH_3)_2$, 72 H), −10.8 (br m, RhHRh, 1 H).

Preparation of $[C_6H_5(H)C{=}C(C_6H_5)(C_6H_5)C{=}CC_6H_5]Rh[P(O\text{-}i\text{-}C_3H_7)_3]_2$. In a typical procedure, 0.20 g (0.19 mmol) of $\{(\mu\text{-H})[P(O\text{-}i\text{-}C_3H_7)_3]_2\}_2$ and 0.10 g (0.56 mmol) of diphenylacetylene were dissolved in approximately 10 mL of toluene. After approximately 10 min, during which the solution changed from dark green to red, the solvent was removed under vacuum. The residue was dissolved in pentane and cooled to −40 °C for 12 h to yield red crystals which contained $(\mu\text{-H})[\mu\text{-}\eta^2\text{-}C_6H_5C{=}C(H)C_6H_5]Rh_2[P(O\text{-}i\text{-}C_3H_7)_3]_4$ as an impurity. Careful recrystallization of the red crystals in pentane at −40 °C led to the isolation of $[C_6H_5(H)C{=}C(C_6H_5)(C_6H_5)C{=}CC_6H_5]Rh[P(O\text{-}i\text{-}C_3H_7)_3]_2$. The yield of the dienyl complex was typically 20%. Anal. Calcd for $C_{46}H_{63}O_6P_2Rh$: C, 63.01; H, 7.24; P, 7.06. Found: C, 63.88; H, 7.38; P, 6.52. The structure of the complex was determined by an X-ray crystallographic study of a single crystal.

Spectroscopic Monitoring of the Reaction of $\{(\mu\text{-H})Rh[P(O\text{-}i\text{-}C_3H_7)_3]_2\}_2$ and 2-Butyne. To a serum-capped NMR tube containing 0.020 g (0.019 mmol) of $\{(\mu\text{-H})Rh[P(O\text{-}i\text{-}C_3H_7)_3]_2\}_2$ in 0.5 mL of toluene-d_8 cooled to −78 °C was added a 0.6 -mL aliquot of vapor (~0.017 mmol of 2-butyne) containing a mixture of N_2 and 2-butyne (*p*(2-butyne) ~ 0.7 atm). The NMR tube was removed from the −78 °C bath and immediately placed in the NMR probe. The resonances of an intermediate species were observed in addition to those of the starting materials and of the ultimate product $(\mu\text{-H})(\mu\text{-}\eta^2\text{-}CH_3C{=}C(H)CH_3)Rh_2[P(O\text{-}i\text{-}C_3H_7)_3]_4$. The resonances of this species were consistent with the formula $(\mu\text{-H})_2(\mu\text{-}\eta^2\text{-}CH_3C{\equiv}CCH_3)Rh_2[P(O\text{-}i\text{-}C_3H_7)_3]_4$: ^1H NMR (toluene-d_8, 20 °C, 250 MHz) δ +4.1 (br m, $CH(CH_3)_2$), +2.15 (br s, $\omega_{1/2} \approx 10$ Hz, $\equiv CCH_3$), +1.40 (d, *J* = 7 Hz, $CH(CH_3)_2$), −10.2 (br t, RhHRh). The resonances for the phosphite ligands of the intermediate overlapped with those for $\{(\mu\text{-H})Rh[P(O\text{-}i\text{-}C_3H_7)_3]_2\}_2$ and $(\mu\text{-H})(\mu\text{-}\eta^2\text{-}CH_3C{=}C(H)\text{-}CH_3)Rh_2[P(O\text{-}i\text{-}C_3H_7)_3]_4$. The resonances for the metal hydride of the intermediate overlapped with those of the product vinyl complex. Conducting the reaction at lower temperature did not produce improved spectra. Continued spectroscopic monitoring at 20 °C showed the complete conversion of all materials to the vinyl complex within ~3–4 min.

Spectroscopic Monitoring of the Reaction of $H(\mu\text{-H})_3Rh_2[P(O\text{-}i\text{-}C_3H_7)_3]_4$ with Excess H_2 and Excess Di-*p*-tolylacetylene. A mixture of 0.020 g (0.019 mmol) of $\{(\mu\text{-H})Rh[P(O\text{-}i\text{-}C_3H_7)_3]_2\}_2$ and 0.010 g (0.049 mmol) of di-*p*-tolylacetylene was dissolved in 0.5 mL of cold toluene-d_8 and quickly transferred to an NMR tube (attached as a sidearm to the reaction vessel) cooled to −196 °C. The tube was charged with 0.5 atm of H_2 (ca. 0.3 mmol; this generates $H(\mu\text{-H})_3Rh_2[P(O\text{-}i\text{-}C_3H_7)_3]_4$ in situ[3]) and sealed. The tube was placed in the NMR probe at 20 °C, and spectra were recorded (the solution was at 20 °C for ~2 min). The ^1H NMR spectrum had resonances of the *p*-tolyl derivatives of *trans*-stilbene, bibenzyl, as well as $(\mu\text{-H})(\mu\text{-}\eta^2\text{-}CH_3C_6H_4C{=}C(H)C_3H_6CH_4)\text{-}Rh_2[P(O\text{-}i\text{-}C_3H_7)_3]_4$. In addition, another species was observed in roughly equal concentration to that of the bridging vinyl complex and was assigned the structure $(\mu\text{-H})_2(\mu\text{-}\eta^2\text{-}CH_3C_6H_4C{\equiv}CC_6H_4CH_3)Rh_2\text{-}[P(O\text{-}i\text{-}C_3H_7)]_4$: ^1H NMR (toluene-d_8, 20 °C, 250 MHz) δ +7.15 (d, Ar CH), +6.8 (d, Ar CH), +5.1 (br m, $CH(CH_3)_2$), +2.15 (s, $C_6H_4CH_3$), +1.38 (d, *J* = 7.0 Hz, $CH(CH_3)_2$), −9.82 (ttt, J_{Rh-H} = 24.0 Hz, J_{P-H} = 11.5 Hz, 91.3 Hz).

Preparation of $\{Rh_2[P(O\text{-}i\text{-}C_3H_7)_3]_4\}_x$. A solution of 0.020 g (0.019 mmol) of $\{(\mu\text{-H})Rh[P(O\text{-}i\text{-}C_3H_7)_3]_2\}_2$ in 10 mL (128 mmol) of 2-butyne was stirred at room temperature in a closed vessel for over 24 h. The 2-butyne was removed by vacuum distillation from the yellow solution to leave a yellow residue. This residue was converted into an orange-yellow powder by cooling a pentane solution (4 mL solvent) to −40 °C. This powder recrystallized from methanol at −40 °C to give orange-yellow crystals. Anal. Calcd for $C_{18}H_{42}O_6P_2Rh$: C, 41.63; H, 8.15; P, 11.93. Found: C, 40.78; H, 8.20; P, 11.64. The powder obtained from pentane and the crystals obtained from methanol gave identical ^1H NMR spectra. ^1H NMR (toluene-d_8, 20 °C, 200 MHz) δ +5.20 (m, $CH(CH_3)_2$, 6 H), +1.40 (d, *J* = 5.9 Hz, $CH(CH_3)_2$, 42 H), −0.40 (s, 1 H). This spectrum was temperature invariant except for the resonance at δ −0.40, which shifted to δ −0.1 at −65 °C. $^{31}P\{^1H\}$ NMR +150 ppm (d, J_{Rh-P} = 200 Hz). This spectrum was temperature invariant from −65 to +20 °C. Reaction of the orange-yellow material with H_2 (1 atm) in toluene gave a mixture of unidentified products that did not appear to contain any $\{(\mu\text{-H})Rh[P(O\text{-}i\text{-}C_3H_7)_3]_2\}_2$.

Procedures for Catalytic Hydrogenation Reactions. Measured amounts of the dialkylalkyne or, for the competition studies, dialkylalkyne and the alkene were prepared by distillation into a graduated tube on a vacuum line. These unsaturated hydrocarbons were then vacuum distilled into a 90-mL reaction tube equipped with a magnetic stir bar and charged with 0.020 g (0.019 mmol) of $\{(\mu\text{-H})Rh[P(O\text{-}i\text{-}C_3H_7)_3]_2\}_2$. The tube and contents were kept cold with liquid nitrogen until H_2 (or D_2) was admitted to 0.8 atm. Only after the hydrogen or deuterium was added was the catalyst and substrate mixture allowed to warm to above liquid nitrogen temperature. The reaction mixture was stirred at room temperature for a predetermined amount of time, and the volatile products were then removed by vacuum distillation. For the studies involving neat 2-butyne, a volume of toluene about 3 times that of the 2-butyne employed was vacuum distilled into the flask containing the product hydrocarbons. This was done in order to lower the partial pressure of the four-carbon hydrocarbons above these solutions and thereby reduce the loss of the products by evaporation during gas chromatographic assay.

The color change associated with the alkyne hydrogenations was from red, (the color of $\{H(\mu\text{-H})_3Rh_2[P(O\text{-}i\text{-}C_3H_7)_3]_4\}$ and also the low-temperature form of $\{(\mu\text{-H})Rh[P(O\text{-}i\text{-}C_3H_7)_3]_2\}_2$), to yellow (rapid) and eventually to red-brown. The color associated with the hydrogenation of internal alkenes was red throughout the reaction while that for terminal alkenes was yellow. At all times in these reactions, the solution appeared homogeneous to visual inspection. After the experiments were complete and the hydrocarbons had been removed, the remaining metal-containing products were found to be completely soluble in pentane; filtration of the solution on a fine porosity frit revealed no detectable particulates.

The hydrocarbon products were assayed by gas chromatography. The relative amounts of each organic product were determined by triangulation of the peaks. Absolute yields of hydrocarbons were determined by using C_6F_6 or mesitylene as internal standards. Subsequent to the hydrogenation reactions with H_2, the organometallic products were dissolved in toluene-d_8 for ^1H NMR spectral studies.

General Procedures for Spectroscopic Monitoring of Reactions. The following procedure was used to monitor rapid reactions spectroscopically. An NMR tube was charged with an appropriate amount of the crystalline rhodium-containing reactant and approximately 0.5 mL of toluene-d_8. Liquid reactants were introduced by vacuum distillation. Hydrogen as

Table I. Details of Data Collection and Least-Squares Refinement for $(\mu\text{-H})[\mu\text{-}\eta^2\text{-}CH_3C_6H_4C{=}C(H)C_6H_4CH_3]Rh_2[P(O\text{-}i\text{-}C_3H_7)_3]_4$ (3b) and $(\mu\text{-H})[\mu\text{-}\eta^2\text{-}CH_3C{=}C(H)CH_3]Rh_2[P(O\text{-}i\text{-}C_3H_7)_3]_4$ (3c)

	3b	3c
cryst system	triclinic, $P\bar{1}, Z = 2$	monoclinic, $P2_1/n, Z = 4$
cell const		
a, Å	12.704 (4)	10.040 (2)
b, Å	12.903 (4)	22.664 (5)
c, Å	21.562 (9)	24.167 (5)
α, deg	91.92 (3)	
β, deg	103.99 (3)	97.58 (2)
γ, deg	109.08 (3)	
V_c, Å^3	3216 (2)	5451 (2)
temp, K	173	153
mol wt, amu	1247.06	1094.86
density, calcd, g/cm^3	1.288	1.334
data collection limit, Å^{-1}	0.538	0.481
data collection scan mode	θ–2θ	ω
total no. of collected rflctns	9123	5888
unique rflctns used in analysis	8418	5075
final agreement factors, $R(F_o)^2$	0.086	0.097
GOF	2.7	1.9
observation to parameter ratio	14:1	10:1

Table II. Details of Data Collection and Refinement for $[C_6H_5(H)C{=}C(C_6H_5)(C_6H_5)C{=}CC_6H_5]$-$Rh[P(O\text{-}i\text{-}C_3H_7)_3]_2\cdot{}^1/_2C_5H_{12}$ (4)

space group	$P\bar{1}, Z = 2$	mol wt, amu	888.9
cell const		density, calcd, g	1.24
a, Å	11.892 (3)	temp, K	138
b, Å	12.455 (4)	final agreement	$R = 0.040$ (5793);
c, Å	18.126 (4)	factors (rflctns)	$R_w = 0.048$ (5793)
α, deg	83.04 (2)	$2\theta_{max}$, deg	45
β, deg	87.33 (2)	GOF	3.1
γ, deg	62.45 (2)	max and min transmission factors	0.916–0.815
V_c, Å^3	2373 (1)	data to parameter ratio	16:1

a reactant was admitted to approximately 0.7 atm, after which the tube was torch sealed and kept at liquid nitrogen temperature until introduction into the NMR probe (probe temperature of −80 °C).

For slower reactions, the toluene-d_8 solutions of the appropriate rhodium complex were added to a serum-capped NMR tube. Additional liquid or gaseous reagents were then added by syringe.

Procedure for High-Pressure Hydrogenation of Diarylalkynes. In a typical procedure, a solution of 0.020 g (0.019 mmol) of $\{(\mu\text{-H})Rh[P(O\text{-}i\text{-}C_3H_7)_3]_2\}_2$ and 0.15 g (0.84 mmol) of diphenylacetylene in 0.75 mL of toluene was added to a glass liner that was then placed inside a 50-mL stainless steel autoclave. (The autoclave manipulations were all performed inside an argon-filled drybox.) Once closed off, the autoclave was removed from the drybox and charged with 1500 psi of H_2. After the appropriate reaction time (at 20 °C), the autoclave pressure was released, and the contents were removed from the autoclave and exposed to air. The products were then analyzed by gas chromatographic assay.

X-ray Data Collection and Structure Solution for $(\mu\text{-H})[\mu\text{-}\eta^2\text{-}CH_3C_6H_4C{=}C(H)C_6H_4CH_3]Rh_2[P(O\text{-}i\text{-}C_3H_7)_3]_4$ (3b) and $(\mu\text{-H})[\mu\text{-}\eta^2\text{-}CH_3C{=}C(H)CH_3]Rh_2[P(O\text{-}i\text{-}C_3H_7)_3]_4$ (3c). After extensive screening, crystals of the two vinyl hydrides (0.25 × 0.27 × 0.25 mm for **3b** and 0.31 × 0.31 × 0.33 mm for **3c**) were chosen for low-temperature data collection. Data were collected by using a Syntex $P2_1$ diffractometer with graphite-monochromated Mo Kα radiation (λ 0.7107Å). Details of data collection and structure refinement are reported in Table I.

Data were corrected for adsorption, Lorentz, and polarization effects, and symmetry related data were averaged. Estimated standard deviations were calculated for each measured intensity according to the equation $\sigma(I) = (I_{total} + I_{bkg}(ST/BT)^2 + (pI)^2)^{1/2}$, where I_{total} and I_{bkg} are the measured total and background intensities, BT and ST are the background and scan times, and $p = 0.02$ for crystal **3b** and 0.05 for crystal **3c**.

The two rhodium and four phosphorus atoms of each molecule were located by using MULTAN.[18] Using phases calculated from the positions of these six atoms, a difference Fourier synthesis revealed the location of all non-hydrogen atoms. These atom positional and thermal parameters were then refined by using a full-matrix least-squares process; anisotropic temperature factors were used for the phosphorus and rhodium atoms. A difference Fourier calculated at this point revealed most of the hydrogen atoms of the isopropyl groups, and the olefinic hydrogen and bridging hydridic atoms were among the highest peaks in the difference map. Because not all the hydrogen atoms of the isopropyl groups were located, none were included in the final cycles of least-squares refinement. In the final least-squares refinements the calculated positional parameters for the phenylic hydrogen atoms were included but not refined. The remainder of the atom parameters were refined by using anisotropic temperature factors, and the least-squares process converged to the agreement factors[19a] reported in Table I.

Scattering factor tables were taken from the International Tables for X-ray Crystallography.[19b] The anomalous scattering contributions of the Rh and P atoms were included in the least-squares refinements. Data collection details and atomic parameters are reported in Tables I, III, and IV.

X-ray Data Collection and Structure Solution for $\{[C_6H_5(H)C{=}C(C_6H_5)(C_6H_5)C{=}CC_6H_5]Rh[P(O\text{-}i\text{-}C_3H_7)_3]_2\}_2\cdot{}^1/_2C_5H_{12}$ (4). A small, well-formed sample of **4** was mounted in a glass capillary and maintained at 138 K with a cold N_2 stream throughout the X-ray crystallographic experiment. Crystal system determination and data collection were performed with a Syntex $P2_1$ autodiffractometer. A least-squares refinement of 23 accurately centered reflections yielded the cell parameters reported in Table II.

The θ–2θ scan mode was employed to collect a hemisphere of data [$(\sin\theta/\lambda)_{max} = 0.54$ Å^{-1}, Mo Kα radiation]. During data collection, three intense reflections were periodically monitored. There were no significant (±3%) fluctuations or trends noted in the intensities of these reflections with exposure time. Data were corrected for Lorentz, polarization, and absorption effects and placed on an absolute scale by means of a Wilson plot. All computations were carried out on a VAX-780 computer with the UCLA crystallographic computing system obtained from Prof. C. Strouse, University of California at Los Angeles.

Statistical methods (MULTAN) were employed to ascertain the Rh and P atomic positional parameters. All non-hydrogen atoms were readily located in subsequent difference Fourier syntheses, including a five-carbon chain centered about an inversion center labeled C(90), C(91), C(92) in Table V. As pentane was employed as the crystallization solvent, this molecule is identified as pentane, C_5H_{12}. At this point, idealized hydrogen atom positions for the phenyl groups were calculated and rigid-body parameters calculated for each C_6H_5 moiety. Full-matrix least-squares refinement commenced with the scale factor, x, y, and z atom positional parameters, isotropic temperature parameters of the non-group atoms, and group positional, rotational, and individual carbon isotropic temperature parameters for the rigid-body types allowed to vary. A difference Fourier synthesis allowed the location of all remaining hydrogen atoms except for those of the C_5H_{12} solvent of crystallization. Least-squares refinement continued as before except all non-hydrogen, non-group atoms were allowed to vary with anisotropic temperature factors. The olefinic hydrogen positional and isotropic thermal parameters were varied, but all other contributions from hydrogen atoms were fixed in the refinement process. After seveal cycles of this least-squaring process, convergence was realized, a difference Fourier synthesis revealed no significant electron density, and structure refinement was therefore halted. Details of data collection and positional parameters are presented in Tables II and V.

Results and Discussion

Catalytic Hydrogenation of Alkynes. It was previously reported that $\{(\mu\text{-H})Rh[P(O\text{-}i\text{-}C_3H_7)_3]_2\}_2$ as a catalyst precursor effected alkene hydrogenation at very high rates.[3] With terminal alkenes, this catalyst yielded turnover rates of about one per second at 20 °C (probably diffusion controlled) while for internal alkenes, the rates were substantially lower, approximately one turnover per minute.[3] The catalyst precursor $\{(\mu\text{-H})Rh[P(O\text{-}i\text{-}C_3H_7)_3]_2\}_2$ underwent no detectable reaction or interaction with alkenes in the absence of hydrogen gas.[3] In the catalytic cycle, the first step was near instantaneous hydrogen addition converting the precursor to the catalytically active intermediate $H(\mu\text{-H})_3Rh_2[P(O\text{-}i\text{-}$

(18) German, G.; Main, P.; Wolfson, M. M. *Acta Crystallogr.* **1965**, *19*, 1014.

(19) (a) Structure solution and initial refinement was accomplished by using CRYM, an amalgamated set of crystallographic computing programs. The remaining details of structure refinement have been reported previously: Teller, R. G.; Williams, J. M. *Inorg. Chem.* **1980**, *19*, 2770. (b) "International Tables for X-Ray Crystallography"; Kynoch Press: Birmingham, England, 1974; Vol. IV.

Table III. Positional[a] Parameters for $(\mu\text{-H})[\mu\text{-}\eta^2\text{-}CH_3C_6H_4C{=}C(H)C_6H_4CH_3]Rh_2[P(O\text{-}i\text{-}C_3H_7)_3]_4$ (3b)

atom	x	y	z
RH(1)	0.65652 (5)	0.19465 (5)	0.29120 (3)
RH(2)	0.46727 (5)	0.24163 (5)	0.20242 (3)
P(1)	0.7213 (2)	0.0588 (2)	0.3177 (1)
P(2)	0.7894 (2)	0.3150 (2)	0.3727 (1)
P(3)	0.4563 (2)	0.4018 (2)	0.2330 (1)
P(4)	0.3065 (2)	0.1913 (2)	0.1223 (1)
O(11)	0.7026 (4)	−0.0410 (4)	0.2635 (2)
O(12)	0.8582 (4)	0.0971 (4)	0.3528 (3)
O(13)	0.6620 (5)	−0.0162 (4)	0.3666 (3)
C(11)	0.7154 (7)	0.0209 (7)	0.1996 (4)
C(111)	0.6201 (8)	−0.1121 (8)	0.1523 (4)
C(112)	0.8363 (8)	−0.0226 (9)	0.1979 (5)
C(12)	0.9135 (7)	0.0359 (7)	0.3983 (4)
C(121)	0.9567 (9)	−0.0397 (9)	0.3626 (5)
C(122)	1.0158 (8)	0.1267 (8)	0.4477 (5)
C(13)	0.632 (1)	−0.1382 (8)	0.3674 (5)
C(131)	0.641 (1)	−0.150 (1)	0.4414 (5)
C(132)	0.520 (1)	−0.1998 (9)	0.3271 (6)
O(21)	0.8055 (4)	0.2784 (4)	0.4450 (2)
O(22)	0.7729 (4)	0.4331 (4)	0.3840 (2)
O(23)	0.9270 (4)	0.3540 (4)	0.3786 (2)
C(21)	0.7049 (7)	0.2130 (8)	0.4657 (4)
C(211)	0.7500 (9)	0.1416 (8)	0.5145 (4)
C(212)	0.6591 (9)	0.291 (1)	0.4971 (5)
C(22)	0.8436 (7)	0.5148 (7)	0.4403 (4)
C(221)	0.9554 (7)	0.5967 (7)	0.4253 (4)
C(222)	0.7628 (8)	0.5760 (8)	0.4539 (5)
C(23)	0.9697 (7)	0.3511 (7)	0.3220 (4)
C(231)	0.9550 (8)	0.4457 (8)	0.2819 (4)
C(232)	1.0987 (8)	0.3665 (9)	0.3474 (5)
O(31)	0.3740 (4)	0.4483 (4)	0.1820 (2)
O(32)	0.574 (5)	0.5066 (4)	0.2552 (3)
O(33)	0.4046 (5)	0.4126 (4)	0.2934 (2)
C(31)	0.3659 (8)	0.5584 (7)	0.1967 (4)
C(311)	0.376 (1)	0.6156 (8)	0.1358 (5)
C(312)	0.248 (1)	0.539 (1)	0.2094 (7)
C(32)	0.6779 (7)	0.5188 (7)	0.2329 (5)
C(321)	0.6509 (8)	0.5067 (8)	0.1594 (4)
C(322)	0.7604 (9)	0.6377 (8)	0.2650 (5)
C(33)	0.4535 (7)	0.3879 (7)	0.3586 (4)
C(331)	0.4520 (9)	0.4775 (9)	0.4040 (4)
C(332)	0.3764 (8)	0.2745 (8)	0.3649 (5)
O(41)	0.2526 (4)	0.0603 (4)	0.1021 (2)
O(42)	0.3093 (4)	0.2270 (4)	0.0521 (2)
O(43)	0.1945 (4)	0.2212 (4)	0.1285 (2)
C(41)	0.1478 (8)	0.0088 (7)	0.0485 (4)
C(411)	0.0800 (8)	−0.1001 (7)	0.0692 (5)
C(412)	0.1831 (9)	−0.0117 (8)	−0.0124 (5)
C(42)	0.3452 (8)	0.3401 (7)	0.0364 (4)
C(421)	0.2363 (9)	0.3662 (9)	0.0055 (5)
C(422)	0.4221 (9)	0.3436 (8)	−0.0096 (5)
C(43)	0.1601 (7)	0.2239 (7)	0.1894 (4)
C(431)	0.1429 (8)	0.1091 (8)	0.2148 (5)
C(432)	0.0459 (7)	0.2465 (8)	0.1675 (5)
C(60)	0.5173 (6)	0.0927 (6)	0.2187 (4)
C(61)	0.5069 (6)	0.1040 (6)	0.1531 (4)
C(62)	0.5942 (6)	0.1655 (6)	0.1205 (3)
C(63)	0.5657 (7)	0.1486 (7)	0.0527 (4)
C(64)	0.641 1 (8)	0.2017 (8)	0.0179 (4)
C(65)	0.7522 (7)	0.2786 (7)	0.0495 (4)
C(66)	0.8376 (8)	0.3356 (9)	0.0127 (5)
C(67)	0.7808 (7)	0.2960 (7)	0.1165 (4)
C(68)	0.7039 (7)	0.2413 (6)	0.1518 (4)
C(69)	0.4228 (6)	0.0086 (6)	0.2356 (3)
C(70)	0.3456 (6)	−0.0890 (6)	0.1934 (4)
C(71)	0.2540 (7)	−0.1618 (7)	0.2109 (4)
C(72)	0.2322 (7)	−0.1453 (7)	0.2694 (5)
C(73)	0.1277 (8)	−0.2270 (8)	0.2889 (5)
C(74)	0.3093 (7)	−0.0543 (7)	0.3133 (4)
C(75)	0.4028 (7)	0.0222 (6)	0.2956 (4)
H	0.580 (8)	0.296 (8)	0.272 (5)
H(61)	0.443 (7)	0.061 (6)	0.126 (4)

[a] x, y, and z are given in fractional coordinates.

Table IV. Positional[a] Parameters for $(\mu\text{-H})[\mu\text{-}\eta^2\text{-}CH_3C{=}C(H)CH_3]Rh_2[P(O\text{-}i\text{-}C_3H_7)_3]_4$ (3c)

atom	x	y	z
RH(1)	0.3378 (1)	0.3672 (0)	0.6406 (0)
RH(2)	0.3799 (1)	0.2580 (0)	0.5839 (0)
P(2)	0.3963 (3)	0.3603 (1)	0.7318 (1)
P(1)	0.3004 (3)	0.4633 (1)	0.6444 (1)
P(4)	0.4409 (4)	0.2316 (2)	0.5037 (1)
P(3)	0.3856 (4)	0.1707 (1)	0.6280 (1)
H	0.391 (6)	0.304 (3)	0.630 (2)
C(59)	0.446 (1)	0.3810 (6)	0.5276 (5)
C(60)	0.345 (1)	0.3414 (6)	0.5527 (5)
C(61)	0.216 (1)	0.3653 (6)	0.5534 (5)
H(61)	0.20	0.407 (5)	0.525 (5)
C(62)	0.094 (1)	0.3276 (6)	0.5613 (6)
O(21)	0.2819 (8)	0.3390 (4)	0.7674 (3)
O(22)	0.5127 (8)	0.3148 (4)	0.7541 (3)
O(23)	0.4371 (8)	0.4193 (3)	0.7658 (3)
C(21)	0.224 (1)	0.2795 (6)	0.7627 (5)
C(211)	0.089 (1)	0.2826 (7)	0.7255 (7)
C(212)	0.214 (2)	0.2625 (7)	0.8230 (6)
C(22)	0.622 (1)	0.2997 (7)	0.7212 (5)
C(221)	0.687 (1)	0.2455 (6)	0.7464 (7)
C(222)	0.724 (1)	0.3511 (7)	0.7270 (8)
C(23)	0.474 (1)	0.4178 (6)	0.8277 (5)
C(231)	0.358 (2)	0.4409 (8)	0.8543 (6)
C(232)	0.599 (2)	0.4579 (7)	0.8405 (6)
O(11)	0.2519 (9)	0.4930 (3)	0.5850 (3)
O(12)	0.4146 (8)	0.5088 (3)	0.6698 (4)
O(13)	0.1907 (8)	0.4849 (3)	0.6817 (3)
C(11)	0.197 (2)	0.5519 (6)	0.5733 (6)
C(111)	0.272 (3)	0.5991 (12)	0.5912 (11)
C(112)	0.183 (4)	0.5517 (8)	0.5087 (8)
C(12)	0.555 (1)	0.5018 (6)	0.6619 (6)
C(121)	0.581 (1)	0.5203 (7)	0.6043 (6)
C(122)	0.636 (2)	0.5374 (8)	0.7085 (6)
C(13)	0.077 (1)	0.4467 (6)	0.6884 (5)
C(131)	−0.040 (1)	0.4597 (6)	0.6432 (6)
C(132)	0.039 (1)	0.4593 (7)	0.7476 (5)
O(41)	0.3582 (9)	0.2544 (4)	0.4455 (3)
O(42)	0.5819 (8)	0.2585 (3)	0.4899 (3)
O(43)	0.4619 (9)	0.1623 (4)	0.4911 (3)
C(41)	0.214 (1)	0.2678 (7)	0.4420 (6)
C(411)	0.191 (2)	0.3243 (6)	0.4087 (7)
C(412)	0.133 (2)	0.2158 (6)	0.4117 (6)
C(42)	0.707 (1)	0.2421 (6)	0.5258 (6)
C(421)	0.817 (1)	0.2393 (6)	0.4871 (6)
C(422)	0.737 (1)	0.2868 (6)	0.5734 (6)
C(43)	0.525 (1)	0.1406 (6)	0.4433 (5)
C(431)	0.415 (2)	0.1234 (7)	0.3954 (6)
C(432)	0.611 (1)	0.0867 (8)	0.4655 (7)
O(31)	0.3160 (8)	0.1717 (4)	0.6839 (4)
O(32)	0.5208 (8)	0.1374 (3)	0.6538 (3)
O(33)	0.3122 (8)	0.1138 (3)	0.5948 (3)
C(31)	0.313 (2)	0.1179 (5)	0.7188 (6)
C(311)	0.413 (1)	0.1240 (6)	0.7710 (5)
C(312)	0.165 (1)	0.1113 (6)	0.7311 (6)
C(32)	0.607 (1)	0.1084 (6)	0.6167 (6)
C(321)	0.584 (2)	0.0415 (6)	0.6199 (6)
C(322)	0.754 (1)	0.1272 (7)	0.6398 (6)
C(33)	0.202 (1)	0.1201 (6)	0.5505 (6)
C(331)	0.204 (2)	0.0648 (6)	0.5149 (6)
C(332)	0.071 (1)	0.1262 (7)	0.5756 (6)

[a] x, y, and z are given in fractional coordinates.

$C_3H_7)_3]_4$. This tetrahydride then reacted rapidly with terminal alkenes at 20 °C to form the corresponding alkane, regenerating $\{(\mu\text{-H})Rh[P(O\text{-}i\text{-}C_3H_7)_3]_2\}_2$. The proposed catalytic cycle is presented in Figure 1.

cis-Alkenes are the typical products of the catalytic hydrogenation of an internal alkyne when the catalyst is a mononuclear metal complex. As noted earlier, coordinately unsaturated polynuclear metal complexes have the potential for stereoselective formation of a *trans*-alkene.[12] This potential was realized for the first time in the catalytic hydrogenation of internal alkynes by $\{(\mu\text{-H})Rh[P(O\text{-}i\text{-}C_3H_7)_3]_2\}_2$. Although the hydrogenation rates were much lower than for terminal alkene hydrogenations, ap-

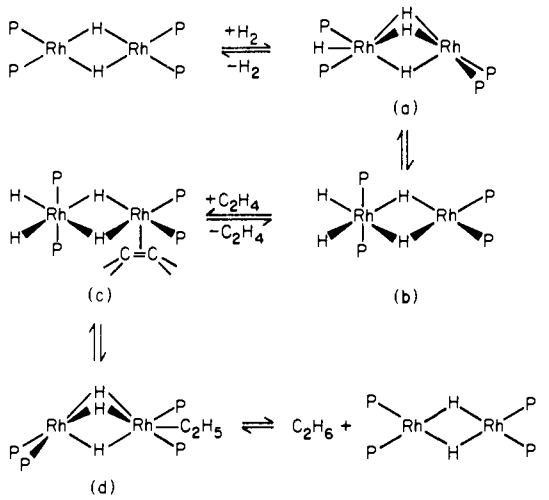

Figure 1. Scheme proposed for the catalytic hydrogenation of alkenes with $\{(\mu\text{-H})\text{Rh}[\text{P}(\text{O-}i\text{-}\text{C}_3\text{H}_7)_3]_2\}_2$ as the catalytic precursor. This scheme is a slightly modified version of the original proposal by Sivak and Muetterties[3] in that intermediates a–d have slightly different stereochemistries. Intermediate b was originally formulated with each phosphite phosphorus atom on the six-coordinate rhodium atom trans to a bridging hydride atom. However, a later crystallographic study of $\mathbf{H}_2(\mu\text{-H})_2\text{Rh}_2[\text{P}(\text{N}(\text{CH}_3)_2)_2)_3]_4$ established[8a] for this species that each terminal hydride ligand, not each phosphorus atom, on the six-coordinate rhodium atom is trans to a bridging hydride atom. An analogous stereochemistry is accordingly employed for b in this modified scheme.

proximately one turnover per minute at 20 °C, the catalytic reaction was totally stereoselective. Unfortunately, catalyst lifetime was very short. After approximately 5 min under the catalytic conditions, *cis*-alkenes became a significant product, and, at long times, the ratio of cis:trans was 95:5 (in the case of diphenylacetylene). This change occurred because the polynuclear catalyst was converted to another catalytically active species that did not yield *trans*-alkenes but rather *cis*-alkenes. This mononuclear species, described below, catalytically converted H_2 and diphenylacetylene to a 95:5 mixture of *cis*-stilbene:*trans*-stilbene.

Mechanistic Features of the Catalytic Alkyne Hydrogenation Reaction. Unlike alkenes, alkynes reacted with $\{(\mu\text{-H})\text{Rh}[\text{P}(\text{O-}i\text{-}\text{C}_3\text{H}_7)_3]_2\}_2$ in the absence of hydrogen to form isolable bridged vinyl complexes $(\mu\text{-H})[\mu\text{-}\eta^2\text{-RC=C(H)R}]\text{Rh}_2[\text{P}(\text{O-}i\text{-}\text{C}_3\text{H}_7)_3]_4$. The reaction rate was low for diarylalkynes such as diphenylacetylene and di-*p*-tolylacetylene: when the molar ratio of diarylalkyne to $\{(\mu\text{-H})\text{Rh}[\text{P}(\text{O-}i\text{-}\text{C}_3\text{H}_7)_3]_2\}_2$ was 1:1, the reaction required approximately 15 min for completion at 20 °C. Reaction rate depended on both the concentration of the dimer and that of the diarylalkyne. For example, when the diarylalkyne was in a 15-fold molar excess, the reaction went to completion in 2–3 min at 20 °C. The rate of reaction of $\{(\mu\text{-H})\text{Rh}[\text{P}(\text{O-}i\text{-}\text{C}_3\text{H}_7)_3]_2\}_2$ with dialkylalkynes was very much faster. Addition of 1 equiv of 2-butyne or 3-hexyne to toluene solutions of the dimer resulted in a near instantaneous reaction. The first-formed product of the reaction of dialkylalkynes with $\{(\mu\text{-H})\text{Rh}[\text{P}(\text{O-}i\text{-}\text{C}_3\text{H}_7)_3]_2\}_2$ was a species whose ^{1}H NMR spectrum was fully consistent with a bridging alkyne complex $(\mu\text{-H})_2(\mu\text{-}\eta^2\text{-RC}\equiv\text{CR})\text{Rh}_2[\text{P}(\text{O-}i\text{-}\text{C}_3\text{H}_7)_3]_4$, analogous to what is typically observed for adducts between alkynes and coordinately unsaturated dimeric metal complexes. Most notably, the alkyne complex had a hydride ^{1}H NMR spectrum that consisted of a triplet of triplet of triplets characteristic of dimeric $(\mu\text{-H})_2(\mu\text{-L}')\text{Rh}_2\text{L}_4$ phosphite complexes and equivalent alkyne substituents (Figure 2). This intermediate then underwent an insertion reaction to form a bridging vinyl complex, $(\mu\text{-H})[\mu\text{-}\eta^2\text{-RC=C(H)R}]\text{Rh}_2[\text{P}(\text{O-}i\text{-}\text{C}_3\text{H}_7)_3]_4$. In contrast, analogous $\mu\text{-}\eta^2$-alkyne intermediates were not detected in the reaction of diarylalkynes with $\{(\mu\text{-H})\text{Rh}[\text{P}(\text{O-}i\text{-}\text{C}_3\text{H}_7)_3]_2\}_2$ perhaps because a significant concentration of this presumed intermediate did not accumulate due to the intrinsically low rate of reaction between the diarylalkynes and the dimer (these intermediates were observed when the starting rhodium complex

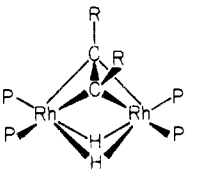

Figure 2. The reaction of dialkylacetylene with $\{(\mu\text{-H})\text{Rh}[\text{P}(\text{O-}i\text{-}\text{C}_3\text{H}_7)_3]_2\}_2$ first forms an alkyne complex that slowly rearranges to form the bridged vinyl complex. This intermediate alkyne complex exhibits ^{1}H and ^{31}P NMR spectra characteristic of $(\mu\text{-H})_2(\mu\text{-L}')\text{Rh}_2[\text{P}(\text{OR})_3]_4$ complexes, e.g., $(\mu\text{-H})_2\text{Rh}_2(\mu\text{-CO})[\text{P}(\text{O-}i\text{-}\text{C}_3\text{H}_7)_3]_4$.[6] On the basis of these spectral data, the alkyne complex is formulated as $(\mu\text{-H})_2(\mu\text{-}\eta^2\text{-RC}\equiv\text{CR})\text{Rh}_2[\text{P}(\text{O-}i\text{-}\text{C}_3\text{H}_7)_3]_4$ with a stereochemistry outlined here (the isopropoxy substituents on the phosphorus atoms are not depicted in the drawing).

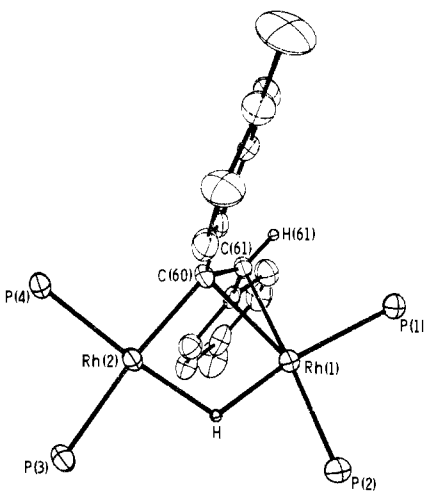

Figure 3. Basic structure of $(\mu\text{-H})[\mu\text{-}\eta^2\text{-RC=C(H)R}]\text{Rh}_2[\text{P}(\text{O-}i\text{-}\text{C}_3\text{H}_7)_3]_4$, with R = $\text{CH}_3\text{C}_6\text{H}_4$. For clarity of stereochemical perspective, the three isopropoxy substituents on each phosphorus atom and the hydrogen atom substituents in the *p*-tolyl groups have been omitted. This view places the two rhodium atoms, the four phosphite phosphorus atoms, the bridging hydride, and the α-vinyl carbon atom, C(60), nearly in the plane of the paper. Note that in an isomeric cis form the phenyl group attached to C(61) would be brought into a significant (repulsive) interaction with the isopropoxy groups (not depicted) of P(1). These same considerations apply to a cis form of the vinyl complex (illustrated in Figure 4) derived from 2-butyne.

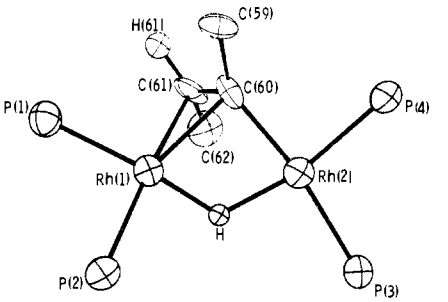

Figure 4. Basic structure of $(\mu\text{-H})[\mu\text{-}\eta^2\text{-CH}_3\text{C=C(H)CH}_3]\text{Rh}_2[\text{P}(\text{O-}i\text{-}\text{C}_3\text{H}_7)_3]_4$ using a perspective view analogous to that employed for the related di-*p*-tolylacetylene-derived vinyl complex (Figure 3). The basic coordination spheres for the two vinyl complexes are strikingly similar and are related as near mirror images.

was $\text{H}(\mu\text{-H})_3\text{Rh}_2[\text{P}(\text{O-}i\text{-}\text{C}_3\text{H}_7)_3]_4$).

The intermediate vinyl complexes were isolated and fully characterized for the diphenylacetylene, di-*p*-tolylacetylene, and 2-butyne derivatives, and the 3-hexyne compound was found spectroscopically to be analogous to the 2-butyne compound. Single crystals of the di-*p*-tolylacetylene- and the 2-butyne-derived compounds were obtained, and low-temperature X-ray crystallographic studies established the structures illustrated in Figures 3 and 4. An analogous structure was defined for the solution state by spectroscopic data. A full discussion of the solid- and

Table V. Positional Parameters[a] for $[C_6H_5(H)C{=}C(C_6H_5)(C_6H_5)C{=}CC_6H_5]Rh[P(O\text{-}i\text{-}C_3H_7)_3]_2 \cdot {}^1/_2C_5H_{12}$ (4)

atom	x	y	z	atom	x	y	z
C(11)	0.1977 (4)	−0.1257 (4)	0.0460 (2)	H(11G)	0.2402 (0)	−0.0463 (0)	−0.0438 (0)
C(111)	0.2076 (5)	−0.2376 (4)	0.0154 (3)	H(11H)	0.0768 (0)	−0.0090 (0)	−0.0412 (0)
C(112)	0.1649 (4)	−0.0206 (4)	−0.0143 (3)	H(12A)	0.4195 (0)	−0.0243 (0)	0.2346 (0)
C(12)	0.5020 (4)	−0.0919 (4)	0.2183 (2)	H(12B)	0.6103 (0)	−0.2482 (0)	0.2705 (0)
C(121)	0.5536 (4)	−0.1855 (4)	0.2859 (2)	H(12C)	0.4965 (0)	−0.2171 (0)	0.3103 (0)
C(122)	0.6002 (4)	−0.0567 (4)	0.1828 (3)	H(12D)	0.5770 (0)	−0.1540 (0)	0.3259 (0)
C(13)	0.5155 (4)	−0.3973 (4)	0.1724 (3)	H(12E)	0.6427 (0)	−0.1043 (0)	0.1652 (0)
C(131)	0.4963 (5)	−0.4571 (4)	0.1098 (3)	H(12F)	0.5617 (0)	0.0046 (0)	0.1440 (0)
C(132)	0.5721 (4)	−0.4873 (4)	0.2407 (3)	H(12G)	0.6139 (0)	−0.0227 (0)	0.2198 (0)
C(21)	0.1043 (4)	−0.2925 (4)	0.2025 (2)	H(13A)	0.5649 (0)	−0.3485 (0)	0.1533 (0)
C(211)	−0.0356 (5)	−0.2156 (4)	0.1856 (3)	H(13B)	0.4686 (0)	−0.4224 (0)	0.0739 (0)
C(212)	0.1490 (5)	−0.4268 (4)	0.1962 (3)	H(13C)	0.4426 (0)	−0.4967 (0)	0.1277 (0)
C(22)	0.3432 (4)	−0.3375 (4)	0.3828 (2)	H(13D)	0.5826 (0)	−0.5225 (0)	0.0947 (0)
C(221)	0.3396 (5)	−0.4585 (5)	0.3933 (3)	H(13E)	0.5839 (0)	−0.4558 (0)	0.2746 (0)
C(222)	0.4159 (5)	−0.3284 (5)	0.4458 (3)	H(13F)	0.6536 (0)	−0.5560 (0)	0.2254 (0)
C(23)	0.0480 (4)	0.1652 (4)	0.5998 (2)	H(13G)	0.5197 (0)	−0.5173 (0)	0.2543 (0)
C(231)	0.0379 (5)	0.1275 (5)	0.5254 (3)	H(21A)	0.1644 (0)	−0.2696 (0)	0.1721 (0)
C(232)	0.1830 (4)	0.1303 (5)	0.6206 (3)	H(21B)	−0.0688 (0)	−0.2497 (0)	0.2124 (0)
C(60)	0.1011 (4)	0.0895 (3)	0.3226 (2)	H(21C)	−0.0478 (0)	−0.2225 (0)	0.1330 (0)
C(61)	0.0199 (3)	0.1475 (3)	0.2608 (2)	H(21D)	−0.0571 (0)	−0.1310 (0)	0.1889 (0)
C(62)	0.0655 (4)	0.2012 (3)	0.1951 (2)	H(21F)	0.1058 (0)	−0.4489 (0)	0.2293 (0)
C(63)	0.1817 (3)	0.1214 (3)	0.1737 (2)	H(21F)	0.1284 (0)	−0.4081 (0)	0.1630 (0)
C(90)	0.0619 (9)	0.4799 (11)	0.5041 (7)	H(21G)	0.2350 (0)	−0.4650 (0)	0.2116 (0)
C(91)	0.0979 (14)	0.5002 (12)	0.5830 (6)	H(22A)	0.3877 (0)	−0.3313 (0)	0.3358 (0)
C(92)	0.1989 (16)	0.4734 (19)	0.5929 (9)	H(22B)	0.2953 (0)	−0.4463 (0)	0.4238 (0)
O(11)	0.3193 (2)	−0.1536 (2)	0.0788 (1)	H(22C)	0.3082 (0)	−0.4694 (0)	0.3601 (0)
O(12)	0.4639 (2)	−0.1426 (2)	0.1607 (1)	H(22D)	0.4327 (0)	−0.5243 (0)	0.3915 (0)
O(13)	0.3910 (2)	−0.3027 (2)	0.1956 (1)	H(22E)	0.3688 (0)	−0.3079 (0)	0.4795 (0)
O(21)	0.1342 (2)	−0.2874 (2)	0.2783 (1)	H(22F)	0.4197 (0)	−0.2490 (0)	0.4411 (0)
O(22)	0.2176 (2)	−0.2370 (2)	0.3817 (1)	H(22G)	0.4966 (0)	−0.4000 (0)	0.4440 (0)
O(23)	0.0005 (2)	−0.1025 (2)	0.3430 (1)	H(23A)	0.0046 (0)	−0.2488 (0)	0.3965 (0)
P(1)	0.3379 (1)	−0.1604 (1)	0.1675 (1)	H(23B)	−0.0263 (0)	0.1582 (0)	0.5107 (0)
P(2)	0.1361 (1)	−0.1696 (1)	0.3058 (1)	H(23C)	0.0793 (0)	0.0672 (0)	0.5321 (0)
Rh	0.1803 (0)	−0.0328 (0)	0.2316 (0)	H(23D)	0.0805 (0)	0.1752 (0)	0.4795 (0)
H(11A)	0.1298 (0)	−0.1019 (0)	0.0847 (0)	H(23E)	0.1848 (0)	0.1483 (0)	0.6622 (0)
H(11B)	0.2293 (0)	−0.3050 (0)	0.0480 (0)	H(23F)	0.2241 (0)	0.0494 (0)	0.6250 (0)
H(11C)	0.1246 (0)	−0.2141 (0)	−0.0045 (0)	H(23G)	0.2205 (0)	0.1728 (0)	0.5765 (0)
H(11D)	0.2715 (0)	−0.2667 (0)	−0.0206 (0)	H(60)	0.0659 (32)	0.0525 (32)	0.3674 (21)
H(11F)	0.1356 (0)	0.0522 (0)	0.0062 (0)				

[a] x, y, and z are given in fractional coordinates.

solution-state structures of these vinyl complexes is presented in the following sections.

The essential point for this stage of the discussion is the stereochemistry of the alkene precursor complex. In $(\mu\text{-H})[\mu\text{-}\eta^2\text{-RC}{=}\text{C(H)R}]Rh_2[P(O\text{-}i\text{-}C_3H_7)_3]_4$ complexes, the unsymmetrically bridging vinyl group has a trans configuration of the original alkyne substituents. Explicably then, reaction of these vinyl complexes with 1 mol of hydrogen yielded the corresponding *trans*-alkene and $\{(\mu\text{-H})Rh[P(O\text{-}i\text{-}C_3H_7)_3]_2\}_2$ as was demonstrated for the stoichiometric and catalytic reaction modes. This stereochemical outcome of the transformation of $(\mu\text{-H})_2(\mu_2\text{-}\eta^2\text{-RC}{\equiv}\text{CR})Rh_2L_4$ to $(\mu\text{-H})[trans\text{-}\mu\text{-}\eta^2\text{-RC}{=}\text{C(H)R}]Rh_2L_4$ phenomenologically accounts for the stereoselective formation of *trans*-alkenes in the catalytic hydrogenation of internal alkynes (see Figure 5[20]). Selective formation (within detection limits) of the trans isomer could be kinetically or thermodynamically controlled. An electronic basis for the selective generation of the trans rather than the cis vinyl derivative is not evident from the experimental data or qualitative theoretical considerations. However, as was noted by a referee, steric factors should substantially favor the trans isomer: in a cis form, the acetylenic R group geminal to the vinylic CH hydrogen atom would encounter substantial repulsive interactions with the isopropoxy substituents of the vicinal phosphite group (Figure 3).

There is a competitive sequence for the catalytic hydrogenation of internal alkynes that comprises initial hydrogen addition to the dimer followed by alkyne reaction as demonstrated by the following experiments. A solution of $H(\mu\text{-H})_3Rh_2[P(O\text{-}i\text{-}C_3H_7)_3]_4$, diphenylacetylene, and hydrogen was allowed to warm in a sealed NMR tube from −78 to +20 °C, and the ^1H NMR spectral changes were monitored then as a function of temperature. Reaction between the alkyne and the tetrahydride began near 0 °C and was relatively fast at +10 °C (much more rapid than the reaction of $\{(\mu\text{-H})Rh[P(O\text{-}i\text{-}C_3H_7)_3]_2\}_2$ and diphenylacetylene), with the only detectable rhodium species at the end of the reaction being the tetrahydride and the stilbenyl complexes. A separate experiment established that the subsequent reaction of the stilbenyl complex with hydrogen to form stilbene and $\{(\mu\text{-H})Rh[P(O\text{-}i\text{-}C_3H_7)_3]_2\}_2$ was slow (see Figure 5). Accordingly, the rate-determining step for the hydrogenation sequence is either the formation of an $H_3(stilbenyl)Rh_2L_4$ species or the reductive elimination of *trans*-stilbene from the implicated trihydridostilbenyl intermediate. Since the catalytic reaction rate was found to be very sensitive to the hydrogen pressure, we presume that the rate-determining step is the addition of hydrogen to the bridging vinyl intermediate.

A reaction competitive with H_2 addition to $(\mu\text{-H})[\mu\text{-}\eta^2\text{-C}_6H_5C{=}\text{C(H)}C_6H_5]Rh_2[P(O\text{-}i\text{-}C_3H_7)_3]_4$, whereby the catalytic products are formed, was shown to be diphenylacetylene addition to the vinyl derivative to form a mononuclear species with two alkyne units per rhodium atom. The mononuclear species is $[R(H)C{=}\overline{C(R)\text{-}(R)C{=}CR}]Rh[P(O\text{-}i\text{-}C_3H_7)_3]_2$, which was isolated in single-crystal form and fully characterized by elemental analysis and single-crystal X-ray diffraction. The molecular

(20) *cis*-Alkenes were stable to the catalytic reaction conditions in that they did not isomerize to the corresponding *trans*-alkene. Monitoring of the catalytic hydrogenation of diphenylacetylene by NMR spectroscopy and by gas chromatographic assay of the organic products showed that *trans*-stilbene was initially the exclusive organic product and that *cis*-stilbene began to appear only as the original catalyst was converted to the new catalytic complex specific for *cis*-alkene formation (approximately 5 min). At this point, the dinuclear vinyl hydride complex was still detectable.

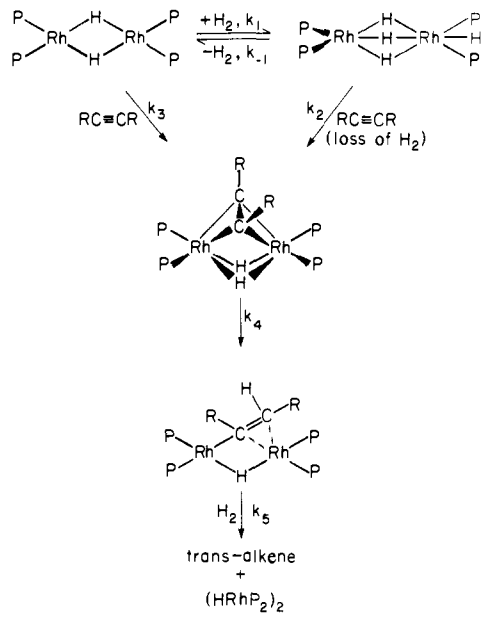

Figure 5. Catalytic sequences whereby internal alkynes are hydrogenated to *trans*-alkenes by the catalyst precursor $\{(\mu\text{-H})Rh[P(O\text{-}i\text{-}C_3H_7)_3]_2\}_2$. All illustrated intermediates were either isolated or structurally defined by spectroscopic data. In addition, the bridged vinyl intermediates were precisely defined by crystallographic analysis (Figures 3 and 4). For dialkylalkynes, k_3k_4 was substantially larger than for diarylalkyne systems starting from the tetrahydride complex. The last sequence, conversion of the bridged vinyl complex to the catalytic end products, probably comprises two elementary steps: hydrogen (H_2) addition followed by hydrogen atom transfer to give the *trans*-alkene and the rhodium dimer. All data suggest that the hydrogen addition step is rate determining. Generally in this partitioned catalytic sequence k_1 is greater than k_3. Exchange studies indicated that formation of the bridged vinyl derivative from the rhodium dimer is reversible.

structure is shown in Figure 8. Formation of this mononuclear complex accounts for the change in the stereoselectivity of the catalytic system, since this species was shown to be a catalyst precursor for the formation of *cis*-stilbene, with *trans*-stilbene accounting for less than 5% of the stilbene product at all stages of the catalytic reaction. Thus, competition of H_2 with diarylalkynes for the key intermediate, the bridging vinyl complex, is the major partitioning step whereby the stereoselective *trans*-alkene formation is diverted to nearly stereoselective *cis*-alkene formation catalyzed by the monomeric complex.

In the 2-butyne catalytic system, there also was conversion of the trans-stereoselective rhodium dimeric species to a new complex that effected a catalytic transformation of the hydrogen and alkyne reactants to *cis*-alkenes, but the new complex was not structurally analogous to that formed in the diarylalkyne systems. The reaction of $\{(\mu\text{-H})Rh[P(O\text{-}i\text{-}C_3H_7)_3]_2\}_2$ with an excess of 2-butyne yielded in addition to the bridging vinyl hydride, a second, nonhydridic, species. This new compound, isolated as yellow crystals, was shown by elemental analysis and ^1H NMR to have the approximate empirical formula $Rh[P(O\text{-}i\text{-}C_3H_7)_3]_2$. This curious complex, which did not react with H_2 (1 atm, 20 °C) to regenerate $\{(\mu\text{-H})Rh[P(O\text{-}i\text{-}C_3H_7)_3]_2\}_2$ or $H(\mu\text{-H})_3Rh_2[P(O\text{-}i\text{-}C_3H_7)_3]_4$, exhibited no metal hydride resonances in the ^1H NMR experiment at temperatures ranging from −65 to +25 °C. The ^1H NMR for the phosphite ligand C−H hydrogen atoms was temperature invariant although there was an additional resonance at δ −0.40, which moved to lower field as the temperature was decreased (at −65 °C, it was at δ −0.10). This unique resonance could arise from some part of an alkyl substituent of the triisopropyl phosphite ligand sufficiently proximate to a metal atom(s) as to effect shielding of some ^1H nuclei. Unfortunately, the mass spectra did not allow a determination of the nuclearity, and all crystals obtained to date have not been suitable for an X-ray diffraction study. Since elemental analysis and the ^1H NMR spectra showed no evidence for the presence of a bound alkyne, the compound appears to be an aggregate of rhodium atoms with two triisopropyl phosphite ligands (or triisopropyl phosphite derived ligands) per rhodium atom. This unresolved structural issue is still under study.

Table VI. Selected Distances (Å)[a] and Angles (deg) in $(\mu\text{-H})[\mu\text{-}\eta^2\text{-}CH_3C_6H_4C{=}C(H)C_6H_4CH_3]Rh_2[P(O\text{-}i\text{-}C_3H_7)_3]_4$ (3b) and $(\mu\text{-H})[\mu\text{-}\eta^2\text{-}CH_3C{=}C(H)CH_3]Rh_2[P(O\text{-}i\text{-}C_3H_7)_3]_4$ (3c)

	3b	3c
(A) Distances within Rhodium Coordination Spheres		
Rh(1)-P(1)	2.205 (2)	2.216 (4)
Rh(1)-P(2)	2.241 (2)	2.213 (4)
Rh(2)-P(3)	2.206 (2)	2.191 (4)
Rh(2)-P(4)	2.220 (6)	2.248 (3)
Rh(1)-H	1.9 (1)	1.56 (6)
Rh(2)-H	1.7 (1)	1.51 (6)
Rh(1)···Rh(2)	2.936 (1)	2.889 (2)
Rh(1)-C(60)	2.226 (8)	2.217 (13)
Rh(2)-C(60)	2.076 (7)	2.049 (15)
Rh(1)-C(61)	2.292 (7)	2.294 (13)
Rh(2)···C(61)	2.998 (8)	2.973 (15)
C(60)···H	2.62 (9)	2.0 (2)
C(60)-C(61)	1.40 (1)	1.40 (1)
C(61)-H(61)	0.87 (7)	1.2 (1)
(B) Average Distances within Phosphite Ligands		
P-O	1.615 (5)	1.608 (8)
O-C	1.47 (1)	1.47 (1)
C-C	1.53 (1)	1.50 (2)
(C) Angles within Rhodium Coordination Spheres		
P(1)-Rh(1)-P(2)	95.2 (1)	93.0 (1)
P(1)-Rh(1)-H	170 (3)	166 (4)
P(1)-Rh(1)-C(6)	107.3 (2)	109.1 (4)
P(2)-Rh(1)-H	90 (3)	93 (2)
P(2)-Rh(1)-C(60)	172.0 (2)	154.1 (4)
C(60)-Rh(1)-H	83 (3)	63 (2)
Rh(1)-H-Rh(2)	108 (5)	139 (4)
Rh(1)-C(6)-Rh(2)	86.0 (3)	85.2 (3)
P(3)-Rh(2)-P(4)	93.3 (2)	100.8 (1)
P(3)-Rh(2)-H	74 (3)	105 (2)
P(3)-Rh(2)-C(60)	154.1 (2)	168.8 (4)
P(4)-Rh(2)-H	168 (3)	146 (3)
P(4)-Rh(2)-C(60)	92.7 (2)	88.8 (4)
C(60)-Rh(2)-H	82 (3)	68 (2)
(D) Average Angles within Phosphite Ligands		
Rh-P-O	118.0 (2)	117.4 (3)
O-P-O	99.7 (3)	99.4 (5)
P-O-C	123.9 (5)	121.8 (7)
O-C-C	107.0 (7)	109.2 (18)

[a] The estimated standard deviation is given for each figure in parentheses.

Crystallographic Investigations of $(\mu\text{-H})[\mu\text{-}\eta^2\text{-}CH_3C_6H_4C{=}C(H)C_6H_4CH_3]Rh_2[P(O\text{-}i\text{-}C_3H_7)_3]_4$ (3b) and $(\mu\text{-H})[\mu\text{-}\eta^2\text{-}CH_3C{=}C(H)CH_3]Rh_2[P(O\text{-}i\text{-}C_3H_7)_3]_4$ (3c). The X-ray crystallographic investigations of $(\mu\text{-H})[\mu\text{-}\eta^2\text{-}CH_3C_6H_4C{=}C(H)C_6H_4CH_3]Rh_2[P(O\text{-}i\text{-}C_3H_7)_3]_4$ (**3b**) and $(\mu\text{-H})[\mu\text{-}\eta^2\text{-}CH_3C{=}C(H)CH_3]Rh_2[P(O\text{-}i\text{-}C_3H_7)_3]_4$ (**3c**) revealed that these two molecules are essentially isostructural. Molecular structures are presented respectively in Figures 3 and 4, stereodiagrams in Figures 9 and 10 of the supplementary material, interatomic distances and angles in Table VI, and least-squares plane calculations in Table VII. Each rhodium atom in **3b** and **3c** has a four-coordinate and nearly coplanar coordination sphere defined by the two phosphorus atoms of the triisopropyl phosphite ligands, the bridging hydride hydrogen atom, and the α-carbon atom of the vinyl ligand. Consistent with this formulation of a four-coordinate, planar $P_2RhH(C)$ primary coordination geometry are the near 90° interligand atom angles (Table VI). The two rhodium atoms, the four phosphite phosphorus atoms, the hydride hydrogen atoms, and the α-carbon atom of the vinyl ligand are very nearly coplanar (Table VII).

There is an unsymmetric bonding of the vinyl ligand in **3b** and **3c**: the α-carbon atom is 0.15 Å closer to one rhodium atom than to the other, specifically 2.076 (7) vs. 2.226 (8) Å for the di-*p*-tolylacetylene derivative and 2.049 (15) vs. 2.217 (13) Å for the 2-butyne derivative. In addition, the β-carbon atom of the vinyl ligand is within bonding distance of the other rhodium atom.

Table VII. Distances (Å) from the Best Least-Squares Planes in $(\mu\text{-H})[\mu\text{-}\eta^2\text{-}CH_3C_6H_4C{=}C(H)C_6H_4CH_3]Rh_2[P(O\text{-}i\text{-}C_3H_7)_3]_4$ (3b) and $(\mu\text{-H})[\mu\text{-}\eta^2\text{-}CH_3C{=}C(H)CH_3]Rh_2[P(O\text{-}i\text{-}C_3H_7)_3]_4$ (3c)

plane	atom	3b	3c
1	Rh(1)	0.095 (1)	−0.126 (1)
	P(1)	−0.046 (2)	0.050 (4)
	P(2)	0.001 (2)	0.006 (3)
	H	−0.05 (11)	0.07 (6)
2	Rh(2)	0.132 (1)	0.078 (1)
	P(3)	−0.087 (2)	−0.169 (4)
	P(4)	−0.002 (2)	0.147 (4)
	H	0.04 (11)	−0.31 (6)
	C(60)	−0.085 (7)	0.26 (1)
3	Rh(1)	0.082 (1)	0.176 (1)
	Rh(2)	0.114 (1)	0.144 (1)
	P(1)	−0.134 (2)	−0.424 (3)
	P(2)	0.075 (2)	0.234 (3)
	P(3)	−0.144 (2)	−0.331 (4)
	P(4)	0.017 (2)	0.341 (4)
	H	−0.01 (11)	−0.14 (6)

Analogous bonding of vinyl ligands has been observed in some triosmium carbonyl clusters (vide infra), but the vinyl ligands in these do not exhibit trans stereochemistry. The rhodium–rhodium separations in **3b** and **3c** are lengthened relative to that in $\{(\mu\text{-H})Rh[P(O\text{-}i\text{-}C_3H_7)_3]_2\}_2$: 2.936 (1) and 2.889 (1) Å, respectively, vs. 2.647 (13) Å for the parent dimer. This lengthening may be due largely to an electronic factor since the vinyl hydride complexes have two more electrons involved in the $Rh(\mu\text{-H})(\mu\text{-vinyl})Rh$ multicenter bonding than does the parent dimer for $Rh(\mu\text{-H})_2Rh$ bonding.

The carbon–carbon bond lengths in the vinyl linkage (1.40 (1) Å for both structures) are understandably longer than in free acetylene (1.34 Å) but also are substantially longer than those in other metal-bound vinyl groups both with and without π bonds to other metal centers. For example, the vinyl carbon–carbon bond length is 1.327 Å in $[C_6H_5(CH_3)C{=}CC_6H_5]Ni[CH_3C(O)CHC(O)CH_3][P(C_6H_5)_3]$[13] and 1.36 (6) Å in $(\mu\text{-H})[(\mu\text{-}\eta^2\text{-}C_6H_5C{=}C(H)C_6H_5]Os_3(CO)_{10}$.[21]

Analysis of the crystallographic results for $(\mu\text{-H})[\mu\text{-}\eta^2\text{-}CR{=}C(H)R]Rh_2[P(O\text{-}i\text{-}C_3H_7)_3]_4$ (R = CH_3 or $C_6H_4CH_3$) revealed a high degree of coplanarity for the bridging vinyl group.[22] This planar geometry seemed surprising because displacement of the alkene substituents away from the metal atom in η^2-alkene metal complexes is a ubiquitous, well-documented phenomenon[23] in which the degree of displacement observed usually correlates well with the π-acceptor ability of the ligand. Since significant electron transfer from Rh(2) to the alkene π^* orbital is suggested by the relatively long C(60)–C(61) bond distance of 1.40 Å[24] in **3b** and **3c**, the near coplanarity of the vinyl coordination groups in these two complexes was all the more unanticipated.

Consideration of Fischer projections of **3c** (R = CH_3) and **3b** (R = $p\text{-}C_6H_4CH_3$) (see Figure 6) suggested a simple explanation for the observed vinyl group planarity. In both molecules, Rh(1), which is regarded as a substituent of the alkene, is tilted *toward* Rh(2) (the Rh(2)–C(61)–C(60)–Rh(1) torsional angles are 76° for **3c** and 75° for **3b**). This is probably a consequence of steric constraints imposed by the bridging hydride ligand. The remaining substituent atoms adopt conformations that maintain strong C(60)–C(61) $p\pi$–$p\pi$ overlap while maximizing bonding overlap between Rh(1) and the π system of the vinyl ligand.

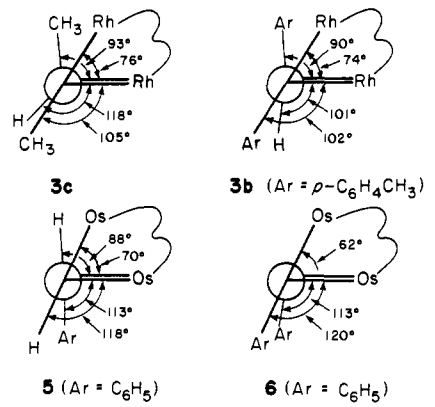

Figure 6. Fischer projections of bridging vinyl complexes viewed along the C–C bond of the bridging ligand. Only the substituents located crystallographically and the value of the associated torsional angles are shown (the locations of the substituents in the figure do not represent the actual torsional angles).

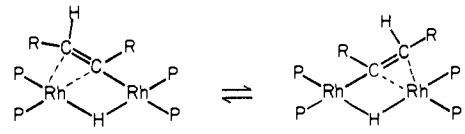

Figure 7. An equilibration that is fast on the NMR time scale at +20 °C and that makes the two rhodium coordination spheres equivalent. The trans relationship of the rhodium and hydride substituents would be maintained through the equilibration process although a process in which cis and trans forms of a vinyl complex would be equilibrated could be operable (although the cis form could not be present in amounts exceeding ~1%).

At least two analogous complexes, $(\mu\text{-H})_3[\mu\text{-}\eta^2\text{-}HC{=}C(H)C_6H_5]Os_4(CO)_{11}$[25] and $(\mu\text{-H})[\mu\text{-}\eta^2\text{-}C_6H_5C{=}C(H)C_6H_5]Os_3(CO)_{10}$,[21,26] have bridging vinyl groups as determined by X-ray crystallographic studies. The Fischer projections of the bridging ligand framework in these two molecules are presented in **5** and **6** of Figure 6 (alkene substituent atoms not located crystallographically are omitted). These projections are remarkably similar to those of **3b** and **3c**, especially in regard to the relative orientations of the two metal atoms bridged by the vinyl group. As with **3b** and **3c**, the apparent planarity of the vinyl coordination groups of **5** and **6** results from the constraints imposed by bonding interactions between the two metal atoms.

Intramolecular and Intermolecular Exchange in the Bridged Vinyl–Rh_2 Complexes. The ^1H NMR spectra at 20 °C of the diphenylacetylene- and di-*p*-tolylacetylene-derived stilbenyl species, **3a** and **3b**, consisted of a metal hydride multiplet, C–H hydrogen resonances for two sets of triisopropyl phosphite ligands with diastereotopic methyl groups, a complex set of resonances for the aryl C–H hydrogen atom (for the di-*p*-tolylacetylene derivatives, these consist of two AB quartets), and a triplet resonance at δ +7.75 for the stilbenyl C–H hydrogen atom (see Experimental Section). Thus,the unique C–H hydrogen atom is equivalently coupled to both rhodium atoms. Additionally, the di-*p*-tolylacetylene derivative showed two resonances for the inequivalent *p*-tolyl methyl group hydrogens. At lower temperatures, ~−20 °C, all four of the phosphite ligands became inequivalent. At this same temperature, the metal hydride resonance had become more complex but had retained its overall triplet character from coupling to the two trans-phosphite ^{31}P nuclei ($J_{P\text{-}H}$ = 74 Hz). In addition, the low-field triplet resonance for the stilbenyl hydrogen had broadened with loss of resolvable ^{103}Rh–^1H coupling ($\omega_{1/2}$ = 20 Hz). Both the metal hydride and the stilbenyl resonances showed

(21) Clauss, A. D.; Tachikawa, M.; Shapley, J. R.; Pierpont, C. G. *Inorg. Chem.* **1981**, *20*, 1528.

(22) A least-squares plane (see Table V) containing C(60), C(61), and the atoms directly bound to them (excluding Rh(2)) showed the vinyl group to be planar, with maximum deviation from the plane of 0.1 Å when R = $p\text{-}CH_3C_6H_4$ and 0.14 Å when R = CH_3.

(23) Ittel, S. D.; Ibers, J. A. *Adv. Organomet. Chem.* **1976**, *14*, 33.

(24) Theoretical calculations of the extended Hückel type were performed on $(PH_3)_4Rh_2(\mu\text{-H})(\mu\text{-}CH{=}CH_2)$ by using the crystallographically determined atom core positions of **3c**. The reduced overlap population between C(60) and C(61) is 1.15 compared to 1.29 found for free ethylene. The reduced overlap populations between Rh(2) and C(60) and also Rh(2) and C(61) were similar (0.13 and 0.08, respectively) while being substantially smaller than that between Rh(1) and C(60) (0.41).

(25) Johnson, B. F. G.; Lewis, J.; Orpen, A. G.; Raithby, P. R.; Rouse, K. D. *J. Chem. Soc., Dalton Trans.* **1981**, 788–792 (combined X-ray and neutron study).

(26) The unit cell of the X-ray crystal structure reported in ref 21 contains two independent molecules. The Fischer projection is derived from the less distorted molecule.

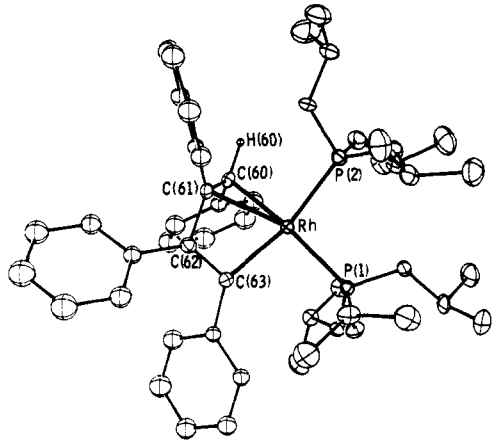

Figure 8. Diarylalkynes can add to the bridged vinyl intermediate in competition with the hydrogen addition depicted for the catalytic cycle (Figure 5). This step is irreversible and leads to the formation of the monomer $[C_6H_5(H)C{=}C(C_6H_5)(C_6H_5)C{=}CC_6H_5]Rh[P(O\text{-}i\text{-}C_3H_7)_3]_2$. The structure of this monomer is shown. To a first approximation, the rhodium atom is four-coordinate, and the four coordinating ligands are nearly coplanar with the rhodium atom, the ligating atoms, or centers are the two phosphite phosphorus atoms, the α-vinyl carbon atom, and the midpoint of the C(60)–C(61) double bond.

some chemical shift temperature dependence; the metal hydride resonance had shifted from δ −11.14 to −11.05, and the stilbenyl resonance had shifted from δ +7.75 to +7.62. All of these spectral changes were fully reversible with respect to change in temperature.

The pattern observed for the −20 °C spectra of the vinyl complexes was consistent with the solid-state structures. The spectral changes observed with temperature increase to +20 °C indicate that the vinyl complexes undergo some intramolecular exchange process that generates a time-averaged mirror plane between the two rhodium centers. One possible process is depicted in Figure 7. Analogous processes have been described for other complexes possessing μ-η^2-vinyl ligands.[27]

Further NMR spectral changes for the vinyl complexes were evident as the temperature was lowered from −18 to −108 °C. Most significant were those of the aryl hydrogen atoms. Additionally, the chemical shifts of the unique stilbenyl C–H and metal hydride resonances continued to change with temperature. At −108 °C, the hydride resonance was at δ −11.0 and the stilbenyl resonance at δ +9.70 (the features of the phosphite resonances, however, were relatively temperature independent over this temperature range). There was no indication that the slow-exchange region for this implied dynamic process was attained even at −108 °C because the substantial rate of change in the Rh–H and stilbenyl C–H resonances had not diminished in the lowest temperature range. All spectral changes were fully reversible. A process that could account for the low-temperature NMR parametric changes is restricted rotation about the stilbenyl C(α) bonds.

The ^{1}H NMR spectrum of the 2-butyne-derived vinyl complex showed similar behavior. At +20 °C, there were two sets of equivalent phosphite ligands. At −65 °C, the spectrum showed the inequivalence of all four phosphite ligands. These spectra are also consistent with the process shown in Figure 7. Because the resonances for the metal hydride and for the vinyl ligand in this complex were much broader than for the diarylalkyne-derived vinyl complex, no substantive information could be derived from these portions of the DNMR spectra.

The NMR spectra of the vinyl complexes presented no evidence for NMR time scale exchange of the vinyl hydrogen atom with the metal hydride either by NMR line shape changes or by the method of spin saturation transfer. However, the alkyne portion of the vinyl ligand is labile. Addition of diarylacetylenes to toluene solutions of $(\mu\text{-H})[trans\text{-}\mu\text{-}\eta^2\text{-}CH_3C{=}C(H)CH_3]Rh_2[P(O\text{-}i\text{-}C_3H_7)_3]_4$ resulted in the generation of free 2-butyne, $(\mu\text{-H})[trans\text{-}\mu\text{-}\eta^2\text{-}CH_3C_6H_4C{=}C(H)C_6H_4CH_3]Rh_2[P(O\text{-}i\text{-}C_3H_7)_3]_4$, and the monomeric rhodium butadienyl complex. Such reactions were complete in approximately 6 h at room temperature. Dissolution of $(\mu\text{-H})[trans\text{-}\mu\text{-}\eta^2\text{-}CH_3C{=}C(H)CH_3]Rh_2[P(O\text{-}i\text{-}C_3H_7)_3]_4$ in toluene resulted in formation of a small proportion of 2-butyne and $\{(\mu\text{-H})Rh[P(O\text{-}i\text{-}C_3H_7)_3]_2\}_2$. In contrast, $(\mu\text{-H})[trans\text{-}\mu\text{-}\eta^2\text{-}C_6H_5C{=}C(H)C_6H_5]Rh_2[P(O\text{-}i\text{-}C_3H_7)_3]_4$ showed no detectable exchange with di-*p*-tolylacetylene at 20 °C in toluene over a 3-day period, although formation of the corresponding monomeric rhodium butadienyl complex was observed.

These experiments demonstrate for the 2-butyne-derived vinyl complex an equilibrium with free butyne and the simple hydride dimer (eq 3). For the analogous diarylalkyne-derived vinyl

$$(\mu\text{-H})[\mu\text{-}\eta^2\text{-}CH_3C{=}C(H)CH_3]Rh_2[P(O\text{-}i\text{-}C_3H_7)_3]_4 \rightleftharpoons CH_3C{\equiv}CCH_3 + \{(\mu\text{-H})Rh[P(O\text{-}i\text{-}C_3H_7)_3]_2\}_2 \quad (3)$$

complexes, the equilibrium must lie far to the left.

X-ray Crystal Structure of $[C_6H_5(H)C{=}C(C_6H_5)(C_6H_5)C{=}CC_6H_5]Rh[P(O\text{-}i\text{-}C_3H_7)_3]_2\cdot{}^1/_2C_5H_{12}$ (4). The structure of $[C_6H_5(H)C{=}C(C_6H_5)\text{-}(C_6H_5)C{=}CC_6H_5]Rh[P(O\text{-}i\text{-}C_3H_7)_3]_2$

Table VIII. Selected Distances (Å) and Angles (deg) in $[C_6H_5(H)C{=}C(C_6H_5)(C_6H_5)C{=}CC_6H_5]Rh[P(O\text{-}i\text{-}C_3H_7)_3]_2\cdot{}^1/_2C_5H_{12}$ (4)

(A) Distances			
Rh-P(1)	2.220 (1)	Rh-P(2)	2.275 (1)
Rh-C(60)	2.225 (4)	Rh-C(61)	2.294 (4)
Rh-C(62)	2.607 (4)	Rh-C(63)	2.081 (4)
C(60)-C(61)	1.407 (5)	C(61)-C(62)	1.496 (5)
C(62)-C(63)	1.357 (5)	C(60)-H(60)	1.05 (3)
P-O (av)	1.613 (3)		
C-C (av)	1.515 (6)		
(B) Angles			
P(1)-Rh-P(2)	98.95 (4)	P(1)-Rh-C(63)	94.1
P(2)-Rh-C(63)	166.1 (1)	P(1)-Rh-mid[a]	163.4 (1)
P(2)-Rh-mid[a]	94.4 (1)	C(63)-Rh-mid[a]	73.1
4(60)-C(60)-phen1[b]	111.1	H(60)-C(60)-C(61)	116 (2)
C(61)-C(60)-phen1[b]	128.1	Rh-C(60)-H(60)	113 (3)
Rh-C(60)-phen1[b]	106.4	C(60)-C(61)-phen2[b]	120.7
C(60)-C(61)-C(62)	118.6 (3)	C(62)-C(61)-phen2[b]	120.4
Rh-C(61)-C(60)	70.6 (2)	Rh-C(61)-C(62)	84.3 (2)
C(61)-C(62)-phen3	119.1	C(63)-C(62)-phen3[b]	129.3
C(61)-C(62)-C(63)	116.1 (3)	Rh-C(63)-phen4[b]	141.6
Rh-C(63)-C(62)	96.3 (1)	C(62)-C(63)-phen4[b]	122.0

[a] Mid refers to the midpoint of the C(60)–C(61) alkene bond. [b] phen1, phen2, phen3, and phen4 refer to the bonded carbon atoms of the phenyl groups 1–4, respectively.

Table IX. Distances from the Best Least-Squares Planes for $[C_6H_5(H)C{=}C(C_6H_5)(C_6H_5)C{=}CC_6H_5]Rh[P(O\text{-}i\text{-}C_3H_7)_3]_2\cdot{}^1/_2C_5H_{12}$ (4)

atom	dist, Å	atom	dist, Å
(A) Rh Atom Coordination Sphere			
Rh	−0.05	P(2)	−0.09
midpoint of C(60)-C(61)	0.15	C(63)	−0.14
P(1)	0.13		
(B) C(60)–C(61) Double Bond and Substituent Atoms			
C(60)	−0.16	phen1	0.24
C(61)	−0.06	phen2	0.21
H(60)	−0.14	C(62)	−0.93
(C) C(62)–C(63) Double Bond and Substituent Atoms			
C(62)	0.00	phen4	0.14
C(63)	−0.01	phen3	−0.20
Rh	−0.21	C(61)	0.28
(D) Four-Carbon Backbone of the Butadienyl Moiety			
C(60)	0.11	C(62)	0.22
C(61)	−0.22	C(63)	−0.11

(27) Shapley, J. R.; Richter, S. I.; Tachikawa, M.; Keister, J. B. *J. Organomet. Chem.* **1975**, *94*, C43.

was determined by low-temperature X-ray crystallography. An ORTEP representation of the structure is presented in Figure 8 and the stereodiagram in Figure 11 of the supplementary material. Selected distances and angles are listed in Table VIII and distances from the best least-squares planes in Table IX. In this complex, the rhodium atom has four-coordinate geometry of ligating ligand atoms, which include the phosphorus atoms of the two triisopropyl phosphite groups, the terminal carbon atom of the butadienyl ligand, and the midpoint (C_2-m) of the terminal alkene carbon atoms in the butadienyl ligand. Structures such as this have been postulated,[28,29] and two have been crystallographically defined.[30,31] The structure of **4** and those of the two related palladium[30] and rhodium[31] heterocyclic structures are very similar even with respect to M-C and C-C distances in the ring portion of the molecules.

The butadienyl ligand is coordinated to the Rh atom through one alkene bond at one end with the phenyl substituents in a trans configuration and through a Rh-C σ bond on the other end with the phenyl substituents of the noncoordinated C=C bond in a cis configuration. The C-C bond distance of the coordinated C=C bond is 1.40 (1) Å, which is close to those of the palladium (1.408 (13) Å) and rhodium (1.428 (7) Å) analogues and which coincides exactly with the corresponding complexed alkene C-C bond distances of the vinyl ligands in the $(\mu\text{-H})[\mu\text{-}\eta^2\text{-RC=C-(H)R}]Rh_2L_4$ complexes discussed above. As expected, the uncomplexed alkene bond distance (1.357 (1) Å) of the butadiene ligand is normal and similar to those in the palladium (1.335 (13) Å) and rhodium (1.348 (7) Å) analogues.

(28) Jack, T. R.; May, C. J.; Powell, J. *J. Am. Chem. Soc.* **1978**, *100*, 5057.
(29) Taylor, S. H.; Maitlis, P. M. *J. Am. Chem. Soc.* **1978**, *100*, 4700.
(30) Bailey, P. M.; Taylor, S. H.; Maitlis, P. M. *J. Am. Chem. Soc.* **1978**, *100*, 4711.
(31) Chang, P.-T.; Nyburg, S. C. *Acta Crystallogr., Sect. B* **1977**, *B33*, 1965.

Conclusions

These studies establish that a unique catalytic reaction can be effected in a polynuclear metal complex in which two (in this instance) or more metal atoms have reactive coordination sites. That the stereoselective catalytic alkyne hydrogenation cycle effected by $\{(\mu\text{-H})Rh[P(O\text{-}i\text{-}C_3H_7)_3]_2\}_2$ is destroyed in a competitive reaction whereby a monomeric complex is formed underscores an oft-described flaw in cluster catalysis, namely, generation of mononuclear metal species. Nevertheless, a principle has been established although utilization of such unique cluster-catalyzed reactions must await design of more robust, catalytically active coordinately unsaturated clusters.

Acknowledgment. This research was supported by the National Science Foundation (Grant CHE 79-03933 to E.L.M. and Grant CHE 78-20698 to J.M.W.). All work at Argonne National Laboratory was performed under the auspices of the Office of Basic Energy Sciences, Division of Materials Sciences of the U.S. Department of Energy. The rhodium used in these studies was obtained on a loan grant from Johnson Matthey, Inc. We also thank the National Science Foundation for a predoctoral fellowship to R.R.B. (1979-1982), the Miller Institute for Research in Science for a grant in the form of a Miller Professorship (E.L.M.) and a Miller Postdoctoral Fellowship (A.J.S.), and the referees for constructive comments.

Registry No. 3a, 82135-60-2; **3b**, 82135-62-4; **3c**, 82135-63-5; **4**, 85354-14-9; $\{(\mu\text{-H})Rh[P(O\text{-}i\text{-}C_6H_7)_3]_2\}_2$, 70727-44-5; $H(\mu\text{-H})_3Rh_2[P(O\text{-}i\text{-}C_3H_7)_3]_4$, 70727-45-6.

Supplementary Material Available: Tables and figures pertaining to the X-ray crystallographic studies of **3b**, **3c**, and **4**, including thermal parameters (Tables X-XIII), calculated and observed structure factors (Tables XIV-XVI), and stereodiagrams (Figures 9-11) (84 pages). Ordering information is given on any current masthead page.

Strain-Reactivity Relations as a Tool for the Localization of Transition States. Equilibria, Solvolysis, and Redox Reactions of Substituted Cycloalkanes[1]

Hans-Jörg Schneider,* Günter Schmidt, and Fred Thomas

Contribution from the Fachrichtung Organische Chemie der Universität des Saarlandes, D 6600 Saarbrücken 11, West Germany. *Received June 17, 1982*

Abstract: MM2 force field calculations are used to obtain strain energy differences ΔSI between sp^2 and sp^3 hybridization states of substituted cycloalkanes with ring size n = 4-12. It is shown that arbitrarily chosen models with substituents such as X = H, OH, CH_3, Hal may lead to a description of steric hindrance around X, instead of $\Delta SI_{sp^2/sp^3}$. If cycloalkanes, which are found largely free from this ambiguity, are analyzed with a proper representation of the multiple reacting conformers, a wide range of reactions, for most of which experimental data are available in the literature, shows satisfactory correlations with sensitivities (slopes) m = 0.1-1.0. For equilibria of ketones (characterized by $\Delta G°_{exp}$) one obtains: with HCN m = 0.97, with H_2SO_3 1.11, with ROH (Meerwein-Ponndorf-Verley isomerization) 0.74. Comparison with ΔG^*_{exptl} for solvolysis of tosylates leads to m = 0.87 in CF_3CH_2OH, to m = 0.69 in AcOH, to m = 0.43 in $EtOH/H_2O$, showing more scatter and less sp^2 character in the more nucleophilic solvents. The contribution to the strain differences ΔSI is ~60% Pitzer strain, ~25% bond angle strain, but only ~3% transannular strain, even for cyclodecanes. The rates of alcohol oxidation with $H_2Cr_2O_7$ (m = 0.13) indicate very early and those of $NaBH_4$ ketone reduction (m = 1.00) extremely late transition states. The results are compared to other mechanistic data, such as to reported stereoselectivities of reductions; they indicate any nonclassical participation in the tosylate solvolysis for cyclobutane to be small ($\Delta\Delta G^* \lesssim 2$ kcal/mol), and for medium rings to be unrecognizable ($\Delta\Delta G^* \lesssim 0.5$ kcal/mol). The correlation of enzymatic (HLADH) reduction rates of cycloalkanones shows considerable scatter, but indicates that the TS is more product- than reactant-like. A necessary revision of the OH orientation in the diamond lattice analysis of the active site is supported by MM2 calculations on axially disubstituted cyclohexanes, which suggest also that nonchair forms need to be considered.

A. Problems and Applications of Strain-Reactivity Calculations. Quantitative relations between steric effects and chemical reactivities hold much promise both for the study of reaction mechanism and for the rational planning, e.g., for stereoselective

0002-7863/83/1505-3556$01.50/0